A purified population of multipotent cardiovascular progenitors derived from primate pluripotent stem cells engrafts in postmyocardial infarcted nonhuman primates.

Guillaume Blin, David Nury, Sonia Stefanovic, Tui Neri, Orianne Guillevic, Benjamin Brinon, Valérie Bellamy, Catherine Rücker-Martin, Pascal Barbry, Alain Bel, et al.

Early Primate Multipotent Cardiovascular Progenitors Derived from Pluripotent Stem Cells Engraft in Postmyocardial Infarcted non Human Primate

Guillaume Blin[1,10,*], David Nury[1,*], Sonia Stefanovic[1,*], Tui Neri[1], Orianne Guillevic[1], Benjamin Brinon[1,2], Valérie Bellamy[2], Catherine Rücker-Martin[3], Pascal Barbry[4], Alain Bel[5], Lionel Bonnevie[6], Patrick Bruneval[5,11], Chad Cowan[7], Julia Pouly[5], Shoukhrat Mitalipov[8], Elodie Gouadon[3], Patrice Binder[9], Albert Hagège[2,5], Michel Desnos[2,5], Jean-François Renaud[3], Philippe Menasché[2,5,12] Michel Pucéat[1,12]

[1]INSERM U633, Avenir program, Embryonic stem cells and cardiogenesis, 91058 Evry, France

[2]INSERM U633, University Paris Descartes, Paris, France

3 CNRS-UMR 8162, Université Paris-Sud, and Hôpital Marie Lannelongue, Le Plessis Robinson, France

[4]Institut de Pharmacologie Moléculaire et Cellulaire, CNRS, Nice, France

[5]Assistance Publique-Hôpitaux de Paris, Hôpital Européen Georges Pompidou, Department of Cardiology (AH and MD), Pathology (PB) and Cardiovascular Surgery (AB,JP,PM);

[6]Department of Cardiology, Hôpital d'Instruction des Armées Bégin, Saint-Mandé, France

[7]Stowers Medical Institute, Center for Regenerative Medicine and Technology, Cardiovascular Research Center, Boston, MA

[8] Division of Reproductive Sciences, Oregon National Primate Research Center, Beaverton, OR, USA.

[9] IMASSA Institut de médecine aérospatiale du service de santé des armées, Brétigny sur Orge, France.

[10] University Montpellier II , France

[11]INSERM U970

[12]To whom correspondence should be addressed: michel.puceat@inserm.fr (33) 1 60 87 89 23 FAX (33) 1 60 87 89 99 INSERM campus genopole 1, 4 rue Pierre Fontaine, EVRY 91058, France or philippe.menasche@egp.aphp.fr (33) 1 56 09 36 22 FAX (33) 1 56 09 32 61 Hopital European Georges Pompidou, 20 rue Leblanc 75015 Paris

[*]These authors listed by alphabetical order equally contributed to the major part of this publication

Conflicts of interest: The authors have declared that no conflict of interest exists

SUMMARY

During embryogenesis, the cardiac cell fate is acquired as early as gastrulation. There is compelling evidence that embryonic stem cells (ESC) can recapitulate early steps in cardiogenesis. Identification from human pluripotent stem cells of early cardiovascular cell progenitors, at the origin of the first cardiac lineage, would shed light on human normal and pathological cardiogenesis and would pave the way toward cell therapy for cardiac degenerative diseases. Here, we report the isolation, and a phenotypic characterisation of an early Oct-4^{+}, SSEA-1^{+}, Mesp1^{+} population of cardiovascular progenitors derived from human pluripotent stem cells. This multipotential progenitor features the capability to generate cardiomyocytes as well as smooth muscle and endothelial cells. We further bring a proof of concept that these progenitors can be used in cardiac regenerative medicine as allografted in infarcted non human primate myocardium, they differentiate in ventricular myocytes without any adverse effect.

Introduction

The embryonic human heart starts beating at around 20 days of gestation and is the target of many genetic and congenital diseases likely originating from the early and complex formation of the myocardium. For the last decades, cardiac progenitors have been tracked in embryos and appeared as a very early lineage determined in the primitive streak of chick (1) as well as of mammals (2) when epiblast cells are incorporated within the posterior primitive streak around day 6 in mouse and 16 in human. Ethical reasons limit the possibility to study such an early stage of development in human embryos. Embryonic stem cells (ESCs) have been long recognised to provide a powerful model to study the early steps of cardiac specification under normal or pathological conditions. Furthermore, ESC-derived cardiomyocytes are a potential cell source for cardiac regeneration. Indeed, cell therapy is a potentially new option for patients with advanced heart failure. However, the clinical trials of bone marrow cells (3) or skeletal myoblasts (MAGIC) transplantation (4) have only yielded marginal results. This has been attributed to the limited plasticity of adult stem cells which precludes their differentiation into functionally integrated cardiomyocytes. Thus, the best substitutes for the missing host cardiomyocytes appear highly plastic cells that can recapitulate cardiomyogenesis. From this standpoint, cardiac stem cells are conceptually attractive but the uncertainties regarding their persistence in adulthood (5) cast serious doubts over their potential therapeutic usefulness. In contrast, pluripotent ESCs emerge as an appealing alternative but so far, their potential use in humans has been hampered by major safety concerns in that, if undifferentiated and injected in immune depressed mice, they generate teratomas. There is also the possibility that a progenitor cell could stop in the course of differentiation and proliferate in an uncontrolled manner *in vivo,* as reported with neuronal progenitors grafted in rat brain (6). Thus, definitively committed, early cardiac progenitors could be the best clinical cell source, in regenerative cardiology. Several groups have

transplanted human (H)ESC-derived cardiomyocytes in post myocardial infarcted rats (7-9). However, as previously discussed (10), fully differentiated cardiomyocytes have a limited number of divisions and an important number of cells would be required to replace those lost as a result of disease. A better option is thus to use cardiac progenitors still capable to divide while differentiating.

Using mouse and HESCs, several cardiac progenitors have been isolated, searching for a common progenitor at the origin of the whole heart (11). Among them, $Isl1^{+}$ multipotent progenitors arising *in vitro* from around embryonic day 8 of differentiation in mouse give rise to different cell lineages presumed to originate from the secondary heart field contributing to two thirds of the myocardium including formation of the right ventricle, part of atria, and the outflow tract but not the contractile left myocardium (12). However, more recently, Isl1 as a marker restricted to the secondary heart field has been challenged (13). Furthermore, as Isl1 is localised in the nucleus of differentiating ES cells and requires embryoid bodies environment to be expressed, these cells cannot be easily sorted in great extent as cardiac precursor cells if one foresees a clinical use. More recently, a population of mouse $Flk1^{+}$ and human $cKit^{-}$, KDR^{low+}, $Nkx2.5^{low+}$, $Isl1^{+}$ cardiovascular cells which is capable to generate up to 57% $cTNT^{+}$ and SMA^{+} cardiomyocytes, in addition to $CD31^{+}$ endothelial and SMA^{+} smooth muscle cells has been identified from a mouse and later a human ES cell line following sequential treatment for 14 days with a cocktail of growth factors including activin, BMP4, FGF2 and VEGF (14, 15). Despite these previous findings, the quest for HESC or induced pluripotent stem (iPS) cell-derived early progenitors at the origin of both the first and secondary cardiac lineages still remains a relevant issue both for basic developmental biology and clinical application.

Here, we have isolated, sorted and characterized such a cell population and we report the feasibility of allograft of primate ESC-derived enriched cardiovascular progenitors in a non-human primate model of myocardial infarction.

Results

Cardiogenic commitment of pluripotent stem cells, generation and sorting of a large and early population of cardiovascular progenitors

To drive HESCs and iPS cells toward a cardiac lineage, we designed experiments to recapitulate the early embryonic developmental pathways from the epiblast stage leading to the precardiac mesoderm lineages. BMP2 together with Wnt3a constitute a potent combination of factors to induce the mesoderm (16, 17). We thus used the cardiogenic morphogen BMP2 in a defined serum free medium and in the presence of the FGF receptor inhibitor SU5402 (18). Such a protocol allowed us to combine the action of BMP2 with the autocrine Wnt3a ligand, whose expression was strongly induced by BMP2 (9±1 fold increase in mRNA expression). The action of secreted Wnt3a was further demonstrated by adding the Wnt inhibitor, dickkopf homolog 1 (DKK) in the presence of BMP2. Indeed, this inhibitor significantly decreased the effect of BMP2 on cardiac gene expression (19) and dramatically reduced the number of cells which lost their pluripotency, and in turn expressed the SSEA-1 antigen (supplemental Figure 1), an index of differentiation of HESCs as well as of the human blastocyst (20). As SSEA-1 is one of the earliest markers of HESC differentiation and loss of pluripotency, and as it is expressed following 4 days treatment of cells with the cardiogenic morphogen BMP2, we reasoned that it might be used to exclude the cells which were not responsive to the morphogen. Indeed, cell sorting using an anti-SSEA-1 antibody allowed to separating cells expressing mRNAs and proteins encoding mesodermal and cardiac markers (21).

We now significantly extended this finding and characterized the genetic and epigenetic profiles of BMP2- and Wnt3a-induced SSEA-1^+ sorted cells as well as their phenotypic fate when engrafted into diseased hearts.

Flow cytometry revealed that 40% (iPS cells) to 53±10% (HESCs, n=15) of BMP2-treated cells stained positive for SSEA-1 (Figure 1A, Table1). Sorting out the BMP2-induced SSEA-1^+ cell population using an antibody coupled to magnetic beads, revealed that these cells still expressed a high level of *Oct-4* mRNA (i.e. above the one required to maintain stem cell pluripotency), an index of their cardiac specification (22) but had lost expression of *Nanog, Crypto or Lefty*, master stem cell pluripotency genes, not expressed in somatic cells. In contrast, the pluripotent stem cell SSEA-1^- population retained expression of these markers (Figure 1B). The BMP2-induced SSEA-1^+ cell population could be sorted out from 5 separate HESC lines, the Rhesus ORMES cell line and iPS with different efficiencies (Table 1).

We next looked at expression of mesodermal and cardiac lineage marker genes by Q-PCR. Freshly sorted SSEA-1^+ cells expressed *Brachyury-T* and *Flk1*, two characteristic genes of the early mesoderm. Furthermore, these cells expressed *Mesp1*, the earliest known marker of cardiopoiesis (23), *Tbx6*, a mesodermal muscle gene upstream of *Mesp1* (24), *Tbx5*, a ventricular marker and *Tbx18*, a marker of both epicardium (25) and the left ventricle (26). SSEA-1^+ cells also expressed *Myocardin, Gata4, Mef2c and Nkx2.5*, key smooth muscle and cardiac transcription factors of the primary heart field as well as *Isl1 and Tbx20,* the latter more reminiscent of the secondary heart field. While expressing *Tbx18*, SSEA-1^+ whole population expressed to a small extent *Nestin* or *Pax3,* two markers found in neural crest cells (Figure 1C). *Tbx3* a marker of the cardiac conduction system (27) among other lineages was not detected (data not shown). We could not either detect any other marker of the hematopoietic or skeletal lineage (CD45, CD34, N-cadherin; MyoD), nor any endodermal (*Sox17, Hex, Foxa*) (data not shown) or ectodermal (*Sox1*) marker. Flow cytometry analysis

confirmed that a minority (5 to 7 % in two separate experiments) of SSEA-1$^+$ cells were Flk1$^+$ at the time of sorting (data not shown). Tbx6 and Mesp1/2 were readily detected in most cells at the level of the protein right after sorting (Fig 1B inset). A similar gene profile could be found in 5 HUES cell lines (HUES-24, HUESC-26, HUES-9, H9, I6) tested.

Gene transcription is tuned by the epigenetic status of stem cells (i.e; the histone code). In ESCs, promoters of transcription factors specific for early cell lineages, feature bivalent domains, harbouring both epigenetic marks, the activating methylation of lysine 4 of histone 3 (H3K4) and the repressive methylation of lysine 27 (H3K27) (28).Thus, to further characterize the BMP2-induced SSEA-1$^+$ cell population, we designed an epigenetic strategy targeting early transcription factors (Figure 1DE). Using chromatin immunoprecipitation assays combined with real-time PCR, we looked at both activating and repressive epigenetic marks on *Oct-4* promoter and on five mesodermal and cardiac promoters. We found that *Oct-4* promoter was associated with an increase in methylation of H3K4 and was occupied by the polymerase II (PolII), two epigenetic marks indicating a transcriptionally active chromatin. *Tbx6, Isl1*, *Mef2c*, *Nkx2.5 and cardiac α-Actin* promoters shared a common epigenetic status, with a thirty to two thousand (*Nkx2.5*) fold increase in PolII occupancy. These data were further confirmed in ChIP experiments using an anti-PolII phosphorylated on serine 5, a better mark of activated bivalent promoters (29) (inset Figure 1E). Ten fold enrichment in H3K4 methylation on cardiac promoters was observed in SSEA-1$^+$ compared to SSEA-1$^-$ cells (Figure 1D) while the H3K27 methylation mark did not significantly change on the same promoters. Interestingly, the promoters of two pluripotency genes *Sox2* and *Nanog* were not any more occupied by serine 5-phosphorylated RNA polymerase II in SSEA-1$^+$ cells (upper Inset Figure 1E). The epigenetic status of *Pax4* promoter an endodermal gene was not changed in SSEA-1$^+$ compared to SSEA-1$^-$ cells.

Early cardiovascular progenitors feature a unique miRNA signature

Besides gene transcription, expression of proteins defining a specific cell fate is also regulated at the posttranscriptional level by small non-coding miRNAs and profiles of miRNAs often reflect a cell-specific signature. We thus used a genomic wide approach (33) to compare the profile of miRNAs in BMP2-induced SSEA-1$^+$ cells and remaining SSEA-1$^-$ or undifferentiated HUES cells. This broad approach showed that SSEA-1$^+$ cells gained expression of specific miRNAs belonging to the cluster miR17-92. These include miR-20a and b known to be turned on when ESCs acquire a cardiac fate (30), miRNAs 17-92 whose downregulation causes a cardiac defect. Furthermore, miRNA 106 whose deletion concomitant to the one of miR 17-92 results in severe cardiac defects (31) was also upregulated in SSEA-1$^+$ cells. MiRNA513, another miRNA not expressed in undifferentiated ESC and whose still unknown functions was highly up-regulated in SSEA-1$^+$ cells; its function is currently under investigation in the laboratory. The gain in expression of these miRNAs were significant in SSEA-1$^+$ cells when compared to the one in SSEA-1$^-$ cells and became even more prominent when compared to the profile of undifferentiated stem cells (Figure 2). MiRNA 302a belonging to the cluster 302 whose expression is regulated by Oct4, and potentially Sox2 and Nanog was also more expressed in SSEA-1$^+$ cells *vs* SSEA1$^-$ cells or HUES cells. This phenomenon could be related to the dual role of this miRNA in both pluripotency and then in specification of HUES cells toward the mesendoderm (32). Another miRNA expressed in HUES cells was also upregulated in SSEA-1$^+$ cells in agreement with its high expression when HUES cells differentiate within embryoid bodies (33). Expression of miRNA 615 and 135 connected to the pluripotency network in ES cells were unchanged (34). Of note the miRNAs 302bcd, also involved in the pluripotency transcriptional network (34, 35) were downregulated in SSEA-1$^+$ cells when compared to SSEA-1$^-$ cells, while they appeared as upregulated when compared to expression level in HUES cells (Figure 2).

The cardiovascular population of SSEA-1$^+$ progenitors is clonogenic and multipotential

To characterize the differentiation potential of SSEA-1$^+$ progenitors towards several cell lineages, we plated isolated SSEA-1$^+$ progenitors as suspensions of single cells on mitotically-arrested Embryonic Day14 Mouse Embryonic Fibroblasts (MEF) in 96 well plates for 5 days, stained them with DAPI and scanned them using an Arrayscan. Despite being plated by limiting dilution at high or low density (5000 down to one single cell/well), cells generated clones within 5 days. The number of clones per well tightly correlated with the starting number of plated cells (Figure 3A). One single cell (monitored by phase contrast microscopy (wild type HUES-24 cell line) or by GFP expression (using the HUES-9 Oct4GFP cell line) was capable to generate a clone within 7 days (Figure 3A, left and coloured right insets). In another set of experiments, a single SSEA-1$^+$ cell was observed while carrying out cytokinesis as early as 2 days post-plating (Figure 3A, inset below the graph). The limiting dilution experiments were confirmed by adding a single cell into a well of a 96 wells plate using a micropipette and by monitoring the formation of a colony (data not shown). Altogether, this demonstrates that SSEA-1$^+$ cells-derived colonies originate from single cells and not from cell clusters, eliminated by thorough trypsinisation and filtering (40μm) before the passage through the sorting magnetic column.

Following one week in culture on MEF in the absence of SU5402, BMP2-induced SSEA-1$^+$ sorted cells-derived colonies still expressed SSEA-1 together with four cardiac-restricted transcription factors, Isl1, Mef2c, Nkx2.5 and Tbx5. A majority of cells from most colonies expressed these markers (Figure 3B) pointing to a rather homogeneous population of cardiac progenitors. Isl1, Mef2c, Nkx2.5 and Tbx5 were all located into the nucleus. Flk1, poorly expressed in freshly sorted SSEA1$^+$ cell population (5-7%) (data not shown), was found later

at the membrane of a proportion but not all cells after one week of culture on feeder cells in the absence of SU5402.

In contrast, HUES-derived SSEA-1$^-$ cells did not express Nkx2.5, Isl1, Mef2c, Tbx5 but still expressed Oct-4, Sox2 and Nanog as assessed by immunofluorescence (data not shown).

Addition of PDGF (10 ng/ml) or VEGF (50 ng/ml), to BMP2-induced SSEA-1$^+$ cells cultured on MEF strongly triggered expression of smooth muscle actin and myosin as well as of CD31 respectively, while only 12% of freshly sorted BMP2-induced SSEA-1$^+$ cells (Supplemental Figure 2A) were CD31$^+$ (Supplemental Figure 2B). Plated on collagen 1-coated dishes, and treated with VEGF (50 ng/ml for 10 days), 80% to 90% of SSEA-1$^+$ cells acquired the morphology of endothelial cells and expressed high level of *CD31*, *CD34*, and *Flk1* mRNAs as well as the protein CD31 for 30 % of them (Supplemental figure 2C) but not cardiac troponin T (data not shown), as investigated by immunofluorescence.

When plated on human fibroblasts in the presence of 5% foetal calf serum or in a mix of human cardiac fibroblasts and cardiomyocytes, 10% and 60% to 80 % of cells, respectively, expressed actinin arranged in sarcomeric units within a week (Figures 3B; 4A). A similar effect was observed in 70% of cells when cells were treated with the conditioned medium of a co culture of human cardiac fibroblasts and cardiomyocytes.

Interestingly, SSEA-1$^+$ cells in culture on MEF for 4 days expressed some genes specific for the secondary heart lineage. This was further enhanced by FGF8 (5 10^{-8}M) (36) treatment of cells for an additional 4 days. FGF8 indeed definitively turned on expression of Tbx1, retinaldehyde dehydrogenase 2 (RALDH2) (37, 38), Hes1 (39) and FoxH1 (40) (Supplemental Figure 3A). FGF8 effect was also observed when genes were monitored at the level of single colonies (data not shown).

To better quantify the cardiogenic fate of BMP2-induced SSEA-1$^+$ cardiovascular progenitors cultured for one week on MEF, immunostained cells cultured in 96 well plates were scored by

High Content Cell imaging (HCCI) using an Arrayscan in two experiments. This technological approach allowed us both to quantify and to visualize cells positive for each cardiac marker. The BMP2-induced SSEA-1^+ population expanded as cardiovascular progenitors within colonies (Figure 3C, right insets) expressed Nkx2.5 and Mef2c (63% and 91% respectively) as well as Isl1 (89%). The cells lost expression of Oct-4 and Sox2 (data not shown). This quantitative analysis by HCCI was confirmed by flow cytometry (data not shown).

To assess the transcriptomic homogeneity of the clones, individual colonies grown for 7 days on MEF were randomly picked-up through a micropipette and screened for gene expression by RT-Q-PCR. These experiments revealed that each colony expressed to a similar and high extent of *Nkx2.5, Mef2c*, cardiac *α-Actin*, *Myocardin* and to a lesser degree *Flk1*. *Isl1* and *Tbx20* were downregulated in 50% of colonies; *Nestin* and *Pax3* were expressed in 50% of clones, actually those expressing *Isl1* and *Tbx20.* None of the colonies expressed Sox17, an endodermal marker (Supplemental Figure 3B). The multipotentiality of a single clone of SSEA-1^+ cells was further demonstrated by cutting single colonies grown on MEF for 5 days into several cell clusters. Cells were then separately replated on collagen 1-coated dishes and treated with PDGF or VEGF or plated on human fibroblasts. In the later case, cardiomyocytes (Supplemental Figure 4A) were observed two to three weeks later, while CD31 (Supplementa Figure 4B) and smooth muscle actin (Supplementa Figure 4C) positive cells were present in growth factor treated cells after one week (Supplementa Figure 4).

In the perspective of a potential use of SSEA-1^+ progenitors in customized regenerative medicine, we used iPS cells. BMP2-induced SSEA-1^+ cells could also be derived from iPS (Supplemental Figure 5A). A similar pattern of expression of cardiac proteins (i.e., Isl1, Mef2c and Nkx2.5) was found in BMP2-triggered SSEA-1^+ cells derived and sorted cells cultured for one week on MEF as assessed by immunofluorescence. Furthermore, a minor

population of BMP2-induced SSEA-1$^+$ iPS (4%) stained positive for CD31 (Supplementa. Figure 5B).

Cardiovascular BMP2-induced SSEA-1$^+$ progenitors differentiate into mature cardiomyocytes ex vivo.

To test the cardiogenicity and the functionality of BMP2-induced SSEA-1$^+$ progenitors prior to animal graft experiments, we used an *ex-vivo* experimental set up. In order to track the fate of cells in culture, Rhesus ES cells (ORMES-2 cell line) were genetically engineered to express GFP under the transcriptional control of the human cardiac α-actin promoter. BMP2-induced SSEA-1$^+$ Rhesus cardiac progenitors were then co-cultured for 4 weeks with human atrial myocytes, cardiac fibroblasts or a mix of cardiomyocytes and fibroblasts (Figure 4). After 4 weeks, microscopic examination revealed the presence of GFP-positive cells (Figure 4) in the three cultures thereby confirming that human cardiac/fibroblastic cells provide the paracrine environment that triggers the cardiomyogenic differentiation of BMP2-induced SSEA-1$^+$ progenitors. The extent of differentiation of BMP2-induced SSEA-1$^+$ cardiac progenitors was prominent and reached 70±10% (in 3 experiments) for cells co-cultured on the mix of cardiac fibroblasts and cardiomyocytes or conditioned medium from the co-culture (Figure 4G). More interestingly, under this experimental situation, a high proportion of cells (60% to 80%), as monitored by concomitant GFP and actinin expression, differentiated in mature cardiomyocytes expressing organised and sarcomeric aligned structures (Figure 4AB). To investigate a potential cell fusion phenomenon, we acquired z-stacks of images (every 200 nm) of BMP2-induced SSEA-1$^+$ cardiac progenitors cultured on a mix of cardiac fibroblasts and cardiomyocytes and stained with an anti-GFP antibody and dapi to visualize the nucleus. Examination of images showed that each GFP cell featured a single nucleus in the same focal

plane (200 nm) as the one where GFP gave the brightest fluorescence (Figure 4B) excluding a fusion with cells sitting below.

No cells were labelled with an anti-SMA antibody. The remaining non- or poorly actinin-positive cells still acquired a cardiac fate as they expressed GFP under the transcritptional control of the cardiac α-actin promoter but failed to set a contractile apparatus. When cultured on myocytes alone, cells remains as foetal (sarcomere size: 1.12±0.02, n=137, 12 cells) (Figure 4C). On fibroblasts, they started to form more mature sarcomeres (1.80±0.03, n=70, 4 cells) (Figure 4D) while on both myocytes and fibroblasts (Figure 4AB), sarcomeres reached an adult size (2.01±0.03, n=127, 10 cells). Furthermore aligned ORMES-derived cardiomyocytes were the only ones to express the ventricular isoform connexin 43 (Cx43) (Figure 4C) at their membrane, the ventricular myosin light chain for 80% of them (Figure 4F) and the adult β-MHC isoform (Figure 4H) for 50% of them, an index of acquisition of an adult ventricular phenotype. When cultured alone on matrigel in the only presence of conditioned medium of a mix of fibroblast and cardiomyocytes, 70% of BMP2-induced SSEA-1^{+} cardiac progenitors adopt a morphology of embryonic cardiomyocytes and developed within two weeks a sarcomeric actin network and became hypertrophied indicating the presence in the conditioned medium of both differentiating and hypertrophic agents (n= 6, Figure 4G). While quiescent as no pacemaker cell was present in the dish, when electrically paced, these cells featured a Ca^{2+}-transient (data not shown). Cx43 was phosphorylated in the cells in contrast to cytosolic microtubule-associated unphosphorylated Cx43, expressed in non mature ORMES-derived cardiomyocytes observed when the latter were cultured on atrial myocytes alone (Figure 4D) or fibroblasts alone (Figure 4E). These data further document that cell transplantation should be performed in the border zone of infarcted myocardium or in patchy scars composed of both fibrosis and reversibly damaged cardiac fibers.

*Cardiovascular BMP2-induced SSEA-1$^+$ progenitors engraft in infarcted primate myocardium and differentiate into mature cardiomyocytes***.**

ORMES cells were treated for 2 days with BMP2. RT-QPCR revealed that BMP2 induced expression of cardiac genes (*Tbx6, Tbx20; Isl1, Mef2c, actin*) (Figure 5A), thereby demonstrating a cardiac print of these cells and confirming the strong cardiac inductive action of BMP2 in non human primate cells. To assess the fate of these cells *in vivo*, we developed a non human primate model of myocardial infarction by subjecting Rhesus monkeys to a percutaneous 90-minute coronary occlusion/reperfusion protocol followed, two weeks later, by open-chest cell transplantation in the infarcted area.

In a first series of pilot experiments, 10^7 BMP2 cardiac-committed cells expressing cardiac genes (Figure 5A) were transplanted in the scar area of 2 immuno-suppressed primates. The primates were euthanized after 2 months. Confocal microscopy of the explanted hearts showed clusters of GFP-positive cells throughout the injected areas within the scar (Figure 5B). Unfortunately, a careful pathological examination of the myocardium and other organs (i.e., lung, liver, …) revealed that 1 out of the 2 primates injected with non-sorted cells had developed a microteratoma in the scar area (Figure 5C). Thus, BMP2-non responsive SSEA-1- and still pluripotent cells proliferated and differentiated within the tumor and should thus be removed before transplantation.

While untreated ORMES featured less than 10% SSEA-1 positive cells, 50±5% of BMP2-challenged cells expressed the antigen (Figure 5D). To confirm the phenotype of SSEA-1$^+$ cells, the gene expression profile of both SSEA-1$^-$ and BMP2-induced SSEA-1$^+$ cell populations was then compared by real time RT-PCR. Figure 5E shows that, as found in HUESC derivatives, the BMP2-induced SSEA-1$^+$ ORMES featured a high expression of *Brachyury, Tbx6, Tbx20, Isl1, Tbx5, Mef2*c and *Nkx2.5* while these genes were barely detectable in the SSEA-1$^-$ cell population. In contrast, BMP2-induced SSEA-1$^+$ cells

dramatically lost expression of most pluripotency genes (i.e., *Crypto, Nanog, Lefty*) in comparison with SSEA-1$^-$ cells (Figure 4E, inset). Of note, *Oct-4* was still expressed at a higher level in BMP2-induced SSEA-1$^+$ than in the SSEA-1-negative cell population as also observed in human BMP2-induced SSEA-1 sorted cells. When cultured on MEF, the SSEA-1$^+$ ORMES sorted cells expressed to a great extent after one week *Tbx20, Isl1, Mef2c, Nkx2.5 and α-actin*. *Brachyury* whose expression was high in freshly sorted cells, was downregulated. The pluripotency genes *Nanog, Lefty, Crypto (TDGF-1) and Oct-4* were all downregulated (Figure 5F).

Infarcted myocardia of 8 immunosuppressed primates were thus transplanted with $2x10^7$ SSEA-1$^+$ cardiac progenitors and 4 with cell medium. The primates were euthanized after 2 and 3 months. Confocal microscopy of the explanted hearts showed clusters of GFP-positive cells throughout the injected areas within the scar (Figure 5H) and this strong cardiac differentiation potential of BMP2-induced SSEA-1$^+$ cardiac progenitors was further confirmed by PCR using GFP-specific primers (data not shown). These cells were surrounded by CD31 and SMA positive cells suggesting either a recruitment of these cells towards the grafted cells or a differentiation of SSEA-1$^+$ cells into these lineages as found *in vitro*. We quantified by imaging GFP and morphometry the extent of the graft within the scar in 60 myocardial sections. The scar area was 284620±82816 μm^2 and the extent of GFP$^+$ cells recolonisation was 65251±46056 μm^2, which represented 20±10% of the scar. The ORMES-derived cardiomyocytes expressed α-actinin, set in sarcomeric structures featuring an adult size (inset) (Figure 5H) and expressing Cx43 (Figure 5H). The ventricular phenotype of these cells was demonstrated by expression of the ventricular isoform of myosin light chain 2 associated with the presence of myosin light chain kinase featuring both diffuse distribution and a sarcomeric organisation (41) (inset Figure 5H). Thus, as shown in a rat model of myocardial infarction (42), the scar environment turned out to be potent enough to trigger

differentiation of cardiac-committed primate ESCs. No teratoma was detectable in any of the 8 primates which had received sorted SSEA1$^+$ cells in any of the investigated organs (myocardium, brain, liver, spleen, pancreas, duodenum, lung, gonads or bones). This finding strongly suggested that some uncommitted SSEA-1$^-$ cells (50% of the injected population), not responsive to BMP2, and thus still undifferentiated pluripotent cells, were at the origin of the tumor, thereby confirming that purification of the progenitor cell population is mandatory for the safety of the procedure. The safety of delivering this SSEA-1$^+$ cell population was further supported by another set of experiments performed in 10 humanized immunodeficient RAG-/-, gamma chain -/-, C5-/- mice which express neither MHC class I and MHC class II genes due to the ablation of the β_2-microglobulin nor I-Aβ^b encoding genes (43). In this series, none of the intracardiac injections of the SSEA-1$^+$, Isl1$^+$, Nkx2.5$^+$, Mef2c$^+$, Tbx5$^+$ cardiac progenitors resulted in teratoma at a four-month follow-up (180 cardiac and other organs sections examined, data not shown).

Discussion

Herein, we have identified a very early population of Oct-4$^+$ cardiac progenitors expressing the membrane antigen SSEA-1. SSEA-1 expression was employed as one of the earliest markers of HUESCs or iPS loss in pluripotency to sort out the cells both responsive and unresponsive to BMP2.

Our findings first revealed that BMP2 in the absence of activin (i.e., in serum-free defined medium) acts in a combinatorial manner with Wnt3a, whose expression was triggered by the morphogen, to drive pluripotent stem cells toward an early mesodermal and cardiogenic fate *in vitro* as expected from both their *in vivo* role in defining the posterior primitive streak and mesoderm (44, 45). Several data suggest that BMP2-induced SSEA1$^+$-sorted cell population is likely to be more reminiscent of the early cardiac progenitors allocated to the epiblast.

When sorted out, these cells still feature a high level of *Oct-4* (i.e, above the level required to maintain cell pluripotency) as confirmed by the epigenetic status (high H3K4 methylation) of its promoter. Despite their early stage of specification, SSEA-1$^+$ Oct-4$^+$ cells acquired a genetic and epigenetic signature, including a profile of miRNA expression, characteristic of pan-cardiac progenitors. They lost pluripotency as indicated by *Nanog*, C*rypto*, *Lefty* and *Sox2* down-regulation concomitantly with the expression of SSEA-1. While the remaining presence of Oct-4 in the absence of other pluripotency genes might be questionable, its level of expression above the one of undifferentiated stem cells also reflects the first step of cell specification toward a cardiogenic fate (19, 22, 46). Such a gene profile together with expression of the proteins Tbx6 and Mesp1/2 indicates that this progenitor somehow reflects the very early cardiac-determined Oct-4$^+$ cell population found in the embryonic epiblast (2, 22). In agreement with the last statement, SSEA1$^+$ cells gained expression of several miRNAs including three (miR-20, miR-17-92, miR 106) reported to be turned on when ESCs acquire a cardiac fate (30) or likely important for mesendodermal differentiation (32) and proliferation of cardiac progenitors (31). Interestingly, miRNAs known to be the major targets of Oct4/Sox2/Nanog transcriptional pluripotency network, miR302s (34, 47, 48) were dramatically down-regulated in SSEA-1$^+$ vs SSEA-1$^-$ cells, supporting the idea that SSEA-1$^+$ cells lost their pluripotency to move along a cardiac differentiation pathway. On the other hand, it could be surprising that SSEA-1$^+$ expressed more mRNAs 302bcd than HUES cells. However, at the time of sorting (when RNAs were extracted for profiling miRNAs), the progenitors still expressed a level of *Oct-4* above the one of HUES cells. As miRNA 302 as well as 135 and 615 are primarily induced by Oct-4 (or lost when Oct-4 is downregulated in the presence of Sox2 and Nanog) (34), this explains that expression of these miRNAs is maintained or even increased. It should be further stressed that their exact role in pluripotency

remains to be established and that as miR106 and 363, they might be involved at later stages in cell lineages differentiation (32, 33).

Finally, when sorted, they express a series of genes (*Brachyury, Tbx6, Mesp, Isl1, Tbx20, Nkx2.5, Mef2c, Myocardin, Tbx18…*) and proteins (Tbx6, Mesp1/2) which altogether, confer them the status of mesodermal cardiogenic cells. Expression of these genes is expected to be sustained as the epigenetic status of their promoter as well as their occupancy by RNA PolII and Phosphorylated Serine5 PolII revealed an active chromatin (H3K4 methylation) and suggest an active transcription, respectively. However, the methylated H3K27 marks still on, indicate a differential regulation of both activating (K4) and repressive marks and that the gain in K4 methylation is sufficient to turn on the promoter as shown by gene transcription. They further acquire in culture the expression of the proteins (Isl1, Nkx2.5, Mef2c, Tbx5 but not SMA) which altogether, indicates that they are cardiac progenitors. Nkx2.5, Isl1, Mef2c and Tbx5 are intranuclear. Tbx5 cellular localization depends upon the stage of cardiac development (49). Thus, its nuclear localisation points that despite the early stage of SSEA-1^{+} cardiac progenitors when sorted, they quickly acquire maturity when in culture.

HCCI together with cell cytometry analysis further revealed that the majority of cells expressed these markers, 70%-90% expressing Isl1, Mef2c, Nkx2.5 proteins. Thus, these findings show that the BMP2-induced SSEA-1^{+} population share some similarities with the recently reported KDR^{+low} cell population (15). However, only 5-7% of BMP2-induced SSEA-1^{+} population is $Flk1^{+}$ (or KDR^{+}) at the level of the protein as assessed by flow cytometry following 4 days of BMP2 treatment, thus suggesting that KDR^{+} cells represent a minor fraction of the sorted SSEA-1^{+} progenitors. As in the KDR^{+low} population (15), c-Kit is also absent from SSEA-1^{+} progenitors as well as from the cardiac field in the embryo (50). However in contrast to KDR^{+low} sorted cells (15), our progenitors do not express SMA if not challenged by PDGF. In fact, our cardiac cell population was sorted out two days earlier than

the KDR^{+low} cells which accounts for the finding that it expresses both Oct4^{+} and Mesp1 proteins, in addition to cardiac-specific markers like Nkx2.5^{+} and Tbx5^{+}, as assessed by HCCI. SSEA-1^{+} Mesp1/2^{+} cardiovascular progenitors also stand much more earlier than the previously isolated Isl1^{+} cells (51) and in contrast to the latter, they feature a great potential to become ventricular myocytes *ex vivo* and when engrafted *in vivo*, what remains to be shown for the Isl1 cells (51). Furthermore our progenitor population was generated using a short protocol (BMP2 inducing Wnt3a) which tends to recapitulate the *in vivo* induction of the primitive streak and subsequently, of cardiogenic mesoderm (17, 44). The most interesting feature of the BMP2-induced SSEA-1^{+} cells is that they retain the capability to differentiate toward the three cardiovascular lineages (i.e., cardiac, endothelial and smooth muscle). When cultured on fibroblasts or a mix of co-cultured human fibroblasts and cardiomyocytes, or in the presence of a conditioned medium of both fibroblasts and cardiomyocytes, they mostly develop a myofibrillogenesis typical of a cardiac cell and express Cx43, MLC2v and βMHC. In contrast, when treated with PDGF or VEGF, they give rise to smooth muscle and endothelial cells, respectively. Thus, these findings point to a multipotentiality of BMP2-induced SSEA-1^{+} cardiovascular progenitors. To further characterize the identity of these cells, we carried out single-clone real time PCR on SSEA-1^{+} cells in culture on embryonic mouse fibroblasts. Interestingly, while most of the clones express pan-cardiac markers (*Mesp1, Nkx2.5, Mef2c, cardiac actin*), 50% expressed *Isl1* and more specifically *Tbx20*, a marker of the secondary heart field suggesting that some Isl1^{+} clones at the level of the protein (Figure 3BC) started to down-regulate expression of this transcription factor while some other kept it. In line with these findings, SSEA-1^{+} cells expressed some of the genes specific for the secondary heart lineage (*Tbx1, RALDH2, Hes1, FoxH1*, Supplemental Figure 3A) and this was dramatically enhanced by FGF8. Isl1^{+} and Tbx20^{+} clones also expressed *Nestin* and *Pax3*, two neural crest and/or stem cell markers and featured the highest level of

Tbx18, which marks both the epicardium (25) and left ventricle (26). These data are in agreement with the interplay between the cardiac neural crest and the secondary heart field (52, 53), a process dependent upon BMP receptors and mediated through neural crest derivatives in the epicardium (54). Alternatively, the Nkx2.5$^+$, Mef2c$^+$, Tbx5$^+$, Tbx20$^+$, Isl1$^+$, Pax3$^+$, Nestin$^+$ population might represent the most multipotent and early precursor (i.e cardiovascular stem cell) population among the SSEA-1$^+$ cells. Interestingly, a similar population was recently described as a cardiac neural crest derived dormant multipotent stem cell in adult heart (55).

Thus, these findings suggest that SSEA-1$^+$ early cardiovascular progenitors, each derived from a single cell (Figure 3A), can segregate into multiple cardiac lineages (primary, secondary heart lineages and potentially cardiac neural crest and epicardium), when challenged by FGFs and other signals emerging from fibroblasts.

The last and very peculiar property of BMP2-induced SSEA-1$^+$ sorted cells is their potential to engraft in a diseased primate myocardium. When replaced *in vivo* in a myocardial environment, they differentiate into mature ventricular cardiomyocytes expressing MLC2v and MLCK required for the assembly of the sarcomeres (56) as expected from their early expression of Tbx5 while retaining a bi- or tri-potentiality to also potentially generate endothelial and smooth muscle cells, although this remains to be confirmed in a xenogenic graft model. They further express Cx43 at their membrane and respond to electrical stimulation suggesting a potential electrical coupling with the neighbouring cells, which remains to be further investigated. Their engraftment turned out to be safe as their status of definite cardiovascular progenitors prevented them from hyperproliferating as confirmed by the absence of formation of teratoma in primate treated with sorted SSEA-1$^+$ cells or in immunodeficient RAG-/- gammaC-/- , C5-/-, MHC -/- humanized mice while SSEA1- still

pluripotent cells gave rise to microteratomas in primate myocardium and huge teratomas in mice.

Altogether, our findings demonstrate that pluripotent stem cells give rise to a single pool of early Oct-4$^+$ and SSEA-1$^+$/brachyury$^+$/Mesp$^+$ cardiogenic mesodermal progenitors. Under specific conditions, the cells further differentiate into cardiac progenitors of the distinct primary and secondary heart lineages or potentially cardiac neural crest expressing *Nkx2.5, Mef2c, Tbx5* with or without *Isl1, Tbx20 and Pax3* and *Nestin.* Finally, challenged with signals derived from cardiac myofibroblasts and adult myocytes, they acquire a fate of differentiated cardiomyocytes. Challenged with other growths factors (PDGF, VEGF), they also acquire the fate of smooth muscle cells expressing smooth muscle actin and myosin, or of early endothelial cells expressing CD31, CD34 and Flk1, respectively.

Thus, we have identified from pluripotent stem cells and characterized a very early cardiovascular progenitor segregating later into the first and second heart lineages (57). Furthermore, we have provided the means to easily sort out this cell population to a great extent. How this population is generated in the cell plates before sorting is likely to be a two-step process. Under BMP2 challenge and in the absence of both FGF (in the presence of SU5402) and activin (in the absence of serum), the Oct-4 up-regulated SSEA-1$^+$ cells go through an endo/mesendodermal fate secreting cardiogenic factors including BMP2 and Wnt3a (19). The latter directs the cells more specifically toward a cardiogenic fate. The cardiac specification is further enhanced in the presence of FGFs (FGF2, FGF4, FGF8…) secreted by MEF while VEGF and PDGF redirect the fate of SSEA-1$^+$ cells towards endothelial and smooth muscle lineages.

Cardiac development is a dynamic process which is tightly orchestrated by the sequential expression of multiple transcription factors working in a combinatory manner. As such, the different cardiac progenitor cell populations described heretofore are not “competitive” but

likely reflect differences in the developmental stage which impact on the nature and extent of the differentiated derivatives in vitro. Within this complex network, the SSEA-1^+ population reported in this paper is appealing because of its ability to give rise to the three main cell lineages of the heart, its user-friendly isolation and its capacity to engraft and to differentiate into mature cardiomyocytes in a clinically relevant large animal model of myocardial infarction. These findings, however, do not preclude that additional studies remain warranted to assess whether still other progenitors might exist which could be endowed with a greater degree of multipotentiality resulting in a correspondingly greater cardiac repair potential.

Acknowledgments:

Guillaume Blin is a fellow from the Ministère de la Recherche et de la Technologie, David Nury and Sonia Stefanovic were funded by the Grants « programme Blanc stem cell signature » and "Specistem" of the National Research Agency (to MP). This study was funded by the National Research Agency (grants Programmes Blanc stem cell signature and Maladies rares to MP), the Genopole Evry, the French Association against Myopathies (AFM grant n°13968 to CR), the LeDucq Foundation (CAPTAA) (Paris to PM and MP), the Foundation Coeur et Artères and the Fonds d'Amorçage des Biothérapies (AP-HP, to PM). Tui Neri is a fellow from the LeDucq Foundation (MITRAL to MP). We thank Laurent Hamon for experimental assistance, Dr S Garcia (Pasteur Institute) for the teratomas formation in mice, Dr P Pradeau, Mr D. Lici and the team of the IMASSA for the care of primates and Daniel Stockholm (Cell Imaging facility, Genethon, Evry) for help in cell imaging.

Methods

Cell Culture. The HUESC lines (HUES-24 and HUES-9 pOct4/GFP from Harvard Stem cell Center) and one human iPS cell line generated using human dermal fibroblasts infected by lentivirus harbouring the cDNAs encoding Oct4, Sox2, Lin 28, Klf4 and nanog (58), were used throughout this study without any difference in results. HUES-24 and HUES-9 pOct4/GFP a transgenic cell line expressing GFP under the transcriptional control of Oct-4 promoter (generated using BAC), and iPS cell lines were cultured on Mouse Embryonic Fibroblasts (MEF) prepared from E14 Mouse embryos using KO-DMEM medium supplemented with β-mercaptoethanol, glutamine, non essential amino acids, 15% KOSR and 10 ng/ml FGF2 respectively.

HUESCs and iPS cells were treated for 4 and 6 (iPS) days with 10 ng/ml BMP2 in the presence of 1 μM SU5402, a FGF receptor inhibitor, in RPMI/B27. HUESCs (both HUES-9 and HUES-24) were used within no more than 10 passages (P28-P38). Cells were phenotyped every 15 passages using anti-SSEA-3/4, TRA-1-60 and TRA-1-80 antibodies (Chemicon). Less than 5 % of cells were positive for SSEA-1 (Chemicon). Karyotype was found normal and stable in the course of the experiments.

Real-Time Quantitative PCR by SYBR Green Detection. RNA was extracted from $SSEA1^+$ or $SSEA1^-$ cells or single clones using Zymo research kits. One μg of RNA or the total RT reaction (single clone) was reverse-transcribed using the Superscript II reverse transcriptase (Invitrogen, Cergy, France) and oligo(16)dT. Q-PCR was performed using a Light Cycler LC 1.5 or 480 (Roche Diagnostic). Amplification and specificity of amplicons was carried out as previously published (19). Data were analysed according to Pfaffl (59).

Cell sorting. Trypsinized cells were incubated for 30 min with anti-SSEA1 antibody-coated Miltenyi beads in D-PBS supplemented with 0.5% (wt/vol) BSA and 2 mM EDTA and transferred to a L50 Miltenyi cartridge set on the magnet. Cells were washed three times with D-PBS- BSA/EDTA and eluted from the column removed from the magnet using 3 ml of D-PBS/BSA/EDTA (19). FACS performed 48Hrs later when beads detached from cells revealed a purity of 95% of SSEA-1^+ cells.

Flow cytometry analysis. BMP2-treated cells were trypsinised and washed twice with PBS, filtered through a 70 μm mesh filter before flow cytometry analysis using FACS Calibur (Becton Dickinson) and CELL QUEST software. Gates were set taken both undifferentiated HUES cells and SSEA-1^- cells stained with both the primary and secondary antibody as negative controls.

Antibodies. The antibodies used for flow cytometry or immunofluorescence were anti-Nkx2.5 (abcam mab2444), anti-Tbx6, Mesp1/2, -Mef2c, (Aviva System biology), anti-Tbx5, anti-MyoD (Abcam) anti-SMA (SMA clone 1A4) and smooth muscle myosin (SMM) (Dako); Anti-Isl1 was from the Developmental Hybridoma bank from Iowa University; the anti-SSEA-1 FITC, anti-CD31, -CD34, and -CD45 were from Beckton Dickinson. The anti MLC2v raised against the specific human myosin light chain residues 45-59 was from Biocytex (France) and the anti MLCK (CloneK36) was from Sigma. Specificity of antibodies was controlled using the respective isotype of the Igs in FACS and using undifferentiated HUESC for immunostaining.

Cell imaging. Confocal microcopy: slides were observed in confocal microscopy (ZEISS LSM510 META) and low power laser allowing to check for the right spectrum of the

fluorochrome that were used (Alexa or GFP) further confirmed by using the META sensitive detector of the LSM510 scanning microscope. A unique feature of the LSM 510 META scan head is its ability to acquire lambda stacks in 10 nm increments over a broad spectral range. GFP was detected within a 520-540 nm window. Some myocardial sections have been also treated to decrease autofluorescence (using NaBH4 treatment of sections). GFP was then labelled by an anti-GFP antibody (Covance) and a secondary Alexa488 or Texas red-conjugated antibody.

High Content Imaging: after immunostaining, 96 well plates were scanned using the Arrayscan (Cellomics ThemoFisher) using the Cell Health Profiling Bioapplication. The fluorescence threshold was determined from the background obtained in undifferentiated HUESCs and set as a fixed threshold value to scan the wells of SSEA1$^+$ cells. 30 fields/well and 18 wells/cardiac markers were scanned as described (19). SSEA-1$^-$ HUESCs stained with the same antibodies as the one used for SSEA1$^+$ cells, were used to set a low and high intensity thresholds independently for each channel (green, red, blue) and exposure parameters (time of exposure 300-600 ms). We also set a background correction. Parameters are saved and all wells are scanned with the same setting**.** The visualisation of images and analysis were then performed using the vHCS software.

Sorted SSEA-1$^+$ cells were plated by limiting dilution into 96 well plates (from 1000 down to a single cell/well), stained 7 days later with DAPI and scanned at 10X magnification using the Health Cell Profiling application from Cellomics. The size and fragmentation of objects were set to identify only clusters of cells (cell colonies). The number of colonies was then scored using the software vHCS (Cellomics).

To ensure that wells contained a single cell, we also used the HUES-9 pOct-4-GFP cell line and monitored the presence of the cell by epifluorescence.

Culture of human fibroblasts and human atrial myocytes

Cells were isolated from right atrial appendage collected during surgery required to relieve congenital diseases from 3-months old patients and cultured as previously described (60). The collection of human tissue is in agreement with the principles outlined by the Ethics Committee of our institution (Committee, protocol 04-26, Hospital at Kremlin Bicêtre, France). Parents of patients provided informed consent prior to their participation in the present study.

Generation of α-actinP-GFP ORMES-2 cell line

10^6 ORMES-2 cells cultured as described above were nucleofected with 3 µg of vector pActin-GFP purified using a Pharmingen kit and linearised. Cells were then cultured on neomycin-resistant MEF for 2 days and G418 (100µg/ml) was added for the next 10 days. Colonies were cut with a needle and picked out of the dish to be further cultured and amplified. Clones were genotyped using GFP primers and further expanded.

Monitoring of gene expression by real time QPCR

To monitor gene expression in separate single clones, single cells-derived colonies grown for 7 days on MEF were picked up randomly using a needle and used for RNA extraction (kit Zymo research). RT-Q-PCR was performed using the LightCycler1.5 as described previously (46) and analysed according to (59).

Chromatin Immunoprecipitation assay was performed according to the Fast ChIP protocol (61). Briefly, cells were crosslinked for 15 min with formaldehyde 1% and the reaction stopped for 5 min by 125 mM glycine. The cell pellet was then washed with cold PBS and the

cells lysed with the ChIP buffer (61). 100 µg Chromatin and 3 µg antibody was used in each assay. The antibodies used were the anti-PolII (santa cruz), anti-Phospho serine5 PolII (Covance) the anti-H3triMeK4, and anti-H3triMeK27 (UBI or Abcam) and were added overnight at 4°C. The Dynabead (protein A conjugated or anti-IgM conjugated (for Phosphoserine 5 PolII, in vitrogen) was used to bind the immunocomplex H3-DNA or PolII-DNA. No antibody and non-relevant rabbit IgG was used as negative controls.

The beads were extensively washed using the ChIP buffer. The protein-DNA interaction was reversed cross-linked by adding chelex to the beads and by boiling the samples for 10 min. DNA was then purified on microcartridges. Q-PCR was used to amplify the DNA using primers specific for promoters (sequence within the 700 bp in 3' of ATG, Table 2). Absolute enrichment was calculated assuming that at most 1% of nucleosomes were immunoprecipitated (62).Genomic region was thus considered enriched if 10 ng IP samples showed a greater enrichment when compared to 0.1 ng of input DNA.

Quantification of the immunoprecipitated DNA was normalized against the starting input material.

MiRNA profiling: Total RNA was extracted from cells using the mirVANA kit (Ambion). 5 µg of RNA for each condition was subjected to dye/swap labelling and was hybridized on printed chips of 2000 mirs originating from 44 species; each spot was done in quadruplet. Raw data were analysed to obtain a log2 intensity value for each spot. Log2 intensity was taken for each spot for both sorted SSEA-1$^+$ cells and control conditions (sorted SSEA-1$^-$ cells or HUESC) and a log2 ratio was obtained. Data were clusterized using Cluster view as previously described (63). The heatmap was generated using Tree view software. Data were validated by real-time PCR. Ten ng of total RNA extracted with mirVana kit were used in a RT reaction using stem-loop microRNA specific primers (Applied biosystem). Subsequently

the diluted RT product was used in a Q-PCR reaction with taqman mir-specific probes. Normalisation was done using small RNA RNU48 as a reference.

Myocardial infarction model

Induction anesthesia of primates was performed with propofol (3mg/kg) and sufentanyl (0.5 mg/kg) and maintenance anesthesia was ensured with the same drugs albeit at a lower dose (1mg/kg and 0.25 mg/kg, respectively). Intravenous atracurium besilate (1mg/kg) was added whenever required and all animals received heparin (50 IU/kg) during the procedure. A myocardial infarction was created in *Macaca Mulatta* Rhesus monkeys (average weight: 8-10 kg) by a 90-minute balloon inflation in the left circumflex coronary artery followed by reperfusion and angiographic confirmation of the patency of the revascularized infarct vessel. The occurrence of myocardial necrosis was consistently documented by a postprocedural rise in creatine phosphokinase values. Two weeks later, primates underwent a left thoracotomy and received 10^7 unsorted or freshly sorted SSEA-1^+ ESC-derived progenitors or just cell medium over the scar and at its borders. The monkeys were treated by either FK-506 started 5 days before cell transplantation at the dose of 1mg/kg/day or by cyclosporine given intramuscularly for 3 days and then by oral gavage at doses adjusted to target serum drug concentrations in the range of 100 ng/mL. Treatments were continued until sacrifice. Primates were humanely euthanized at 2 and 3 months after transplantation. The area of infarction and cell grafting was identified by sutures that had been placed circumferentially at the time of cell injections. This area was cut into two halves, of which one was used for assessment for teratoma. The second half was divided into four blocks which were snap-frozen in isopentane cooled in liquid nitrogen and subsequently processed as cryosections for identification and characterization of GFP^+ grafted cells. In addition, a whole-body autopsy was performed in each animal and used for the search for extracardiac tumors. The experiments with primates

were authorized by the Institutional Review Board on Ethics for primate experiments, in IMASSA at Brétigny-sur-Orge, France

Cell transplantation in immunosuppressed mice

10^5 BMP2-induced SSEA1$^+$ cells were injected in the myocardium (n=8) after opening the chest or subcutaneously in the neck (n=10) of immunodeficient RAG-/- gammaC-/- C5-/- humanized mice. Undifferentiated cells and SSEA1$^-$ cells were also injected subcutaneously in the neck (n=5 each group). Four months later, the animals were euthanized and each organ was collected, sliced and examined for the presence of tumor.

Statistics. Results are presented as mean ± SEM of 3 to 8 experiments in each experimental conditions. Significance of data was evaluated by a Student-t-test. A p value of 0.05 was considered significant. (* $p \leq 0.05$, ** $p \leq 0.01$)

References

1. Rudnick, D. 1938. Differentiation in culture of pieces of early chick blastoderm. *Ann. N.Y.Acad. Sci.* 49:761–772.
2. Tam PPL, and Schoenwolf, G. 1999. Cardiac fate map: lineage, allocation, morphogenetic movement and cell commitment. *Heart Development*:3-18.
3. Hendrikx, M., Hensen, K., Clijsters, C., Jongen, H., Koninckx, R., Bijnens, E., Ingels, M., Jacobs, A., Geukens, R., Dendale, P., et al. 2006. Recovery of regional but not global contractile function by the direct intramyocardial autologous bone marrow transplantation: results from a randomized controlled clinical trial. *Circulation.* 114:I101-107.
4. Menasche, P., Alfieri, O., Janssens, S., McKenna, W., Reichenspurner, H., Trinquart, L., Vilquin, J.T., Marolleau, J.P., Seymour, B., Larghero, J., et al. 2008. The Myoblast Autologous Grafting in Ischemic Cardiomyopathy (MAGIC) trial: first randomized placebo-controlled study of myoblast transplantation. *Circulation.* 117:1189-1200.
5. Pouly, J., Bruneval, P., Mandet, C., Proksch, S., Peyrard, S., Amrein, C., Bousseaux, V., Guillemain, R., Deloche, A., Fabiani, J.N., et al. 2008. Cardiac stem cells in the real world. *J Thorac Cardiovasc Surg.* 135:673-678.
6. Roy, N.S., Cleren, C., Singh, S.K., Yang, L., Beal, M.F., and Goldman, S.A. 2006. Functional engraftment of human ES cell-derived dopaminergic neurons enriched by coculture with telomerase-immortalized midbrain astrocytes. *Nat Med.* 12:1259-1268.
7. Laflamme, M.A., Chen, K.Y., Naumova, A.V., Muskheli, V., Fugate, J.A., Dupras, S.K., Reinecke, H., Xu, C., Hassanipour, M., Police, S., et al. 2007. Cardiomyocytes derived from human embryonic stem cells in pro-survival factors enhance function of infarcted rat hearts. *Nat Biotechnol* 25:1015-1024.
8. Caspi, O., Huber, I., Kehat, I., Habib, M., Arbel, G., Gepstein, A., Yankelson, L., Aronson, D., Beyar, R., and Gepstein, L. 2007. Transplantation of human embryonic stem cell-derived cardiomyocytes improves myocardial performance in infarcted rat hearts. *J Am Coll Cardiol.* 50:1884-1893.
9. van Laake, L.W., Passier, R., Doevendans, P.A., and Mummery, C.L. 2008. Human embryonic stem cell-derived cardiomyocytes and cardiac repair in rodents. *Circ Res.* 102:1008-1010.
10. Passier, R., van Laake, L.W., and Mummery, C.L. 2008. Stem-cell-based therapy and lessons from the heart. *Nature.* 453:322-329.
11. Garry, D.J., and Olson, E.N. 2006. A common progenitor at the heart of development. *Cell.* 127:1101-1104.
12. Moretti, A., Caron, L., Nakano, A., Lam, J.T., Bernshausen, A., Chen, Y., Qyang, Y., Bu, L., Sasaki, M., Martin-Puig, S., et al. 2006. Multipotent embryonic isl1+ progenitor cells lead to cardiac, smooth muscle, and endothelial cell diversification. *Cell.* 127:1151-1165.
13. Ma, Q., Zhou, B., and Pu, W.T. 2008. Reassessment of Isl1 and Nkx2-5 cardiac fate maps using a Gata4-based reporter of Cre activity. *Dev Biol* 22:22.
14. Kattman, S.J., Huber, T.L., and Keller, G.M. 2006. Multipotent flk-1+ cardiovascular progenitor cells give rise to the cardiomyocyte, endothelial, and vascular smooth muscle lineages. *Dev Cell.* 11:723-732.
15. Yang, L., Soonpaa, M.H., Adler, E.D., Roepke, T.K., Kattman, S.J., Kennedy, M., Henckaerts, E., Bonham, K., Abbott, G.W., Linden, R.M., et al. 2008. Human cardiovascular progenitor cells develop from a KDR+ embryonic-stem-cell-derived population. *Nature.* 453:524-528.

16. Crease, D.J., Dyson, S., and Gurdon, J.B. 1998. Cooperation between the activin and Wnt pathways in the spatial control of organizer gene expression. *Proc Natl Acad Sci U S A.* 95:4398-4403.
17. Bakre, M.M., Hoi, A., Mong, J.C., Koh, Y.Y., Wong, K.Y., and Stanton, L.W. 2007. Generation of multipotential mesendodermal progenitors from mouse embryonic stem cells via sustained Wnt pathway activation. *J Biol Chem.* 282:31703-31712.
18. Tomescot, A., Leschik, J., Bellamy, V., Dubois, G., Messas, E., Bruneval, P., Desnos, M., Hagege, A.A., Amit, M., Itskovitz, J., et al. 2007. Differentiation in vivo of cardiac committed human embryonic stem cells in postmyocardial infarcted rats. *Stem Cells.* 25:2200-2205.
19. Stefanovic, S., Abboud, N., Desilets, S., Nury, D., Cowan, C., and Puceat, M. 2009. Interplay of Oct4 with Sox2 and Sox17: a molecular switch from stem cell pluripotency to specifying a cardiac fate. *J. Cell. Biol* 186:665-673.
20. Henderson, J.K., Draper, J.S., Baillie, H.S., Fishel, S., Thomson, J.A., Moore, H., and Andrews, P.W. 2002. Preimplantation human embryos and embryonic stem cells show comparable expression of stage-specific embryonic antigens. *Stem Cells.* 20:329-337.
21. Leschik, J., Stefanovic, S., Brinon, B., and Puceat, M. 2008. cardiac comitment of primate embryonic stem cells. *Nature Protocols* 3:1381-1387.
22. Stefanovic, S., and Puceat, M. 2007. Oct-3/4: not just a gatekeeper of pluripotency for embryonic stem cell, a cell fate instructor through a gene dosage effect. *Cell Cycle.* 6:8-10.
23. Bondue, A., Lapouge, G., Paulissen, C., Semeraro, C., Iacovino, M., Kyba, M., and Blanpain, C. 2008. Mesp1 acts as a master regulator of multipotent cardiovascular progenitor specification. *Cell Stem Cell.* 3:69-84.
24. Christiaen, L., Stolfi, A., Davidson, B., and Levine, M. 2009. Spatio-temporal intersection of Lhx3 and Tbx6 defines the cardiac field through synergistic activation of Mesp. *Dev Biol.* 328:552-560.
25. Cai, C.L., Martin, J.C., Sun, Y., Cui, L., Wang, L., Ouyang, K., Yang, L., Bu, L., Liang, X., Zhang, X., et al. 2008. A myocardial lineage derives from Tbx18 epicardial cells. *Nature.* 454:104-108.
26. Franco, D., Meilhac, S.M., Christoffels, V.M., Kispert, A., Buckingham, M., and Kelly, R.G. 2006. Left and right ventricular contributions to the formation of the interventricular septum in the mouse heart. *Dev Biol.* 294:366-375.
27. Horsthuis, T., Buermans, H.P., Brons, J.F., Verkerk, A.O., Bakker, M.L., Wakker, V., Clout, D.E., Moorman, A.F., t Hoen, P.A., Christoffels, V.M., et al. 2009. Gene expression profiling of the forming atrioventricular node using a novel tbx3-based node-specific transgenic reporter. *Circ Res.* 105:61-69.
28. Bernstein, B.E., Mikkelsen, T.S., Xie, X., Kamal, M., Huebert, D.J., Cuff, J., Fry, B., Meissner, A., Wernig, M., Plath, K., et al. 2006. A bivalent chromatin structure marks key developmental genes in embryonic stem cells. *Cell.* 125:315-326.
29. Stock, J.K., Giadrossi, S., Casanova, M., Brookes, E., Vidal, M., Koseki, H., Brockdorff, N., Fisher, A.G., and Pombo, A. 2007. Ring1-mediated ubiquitination of H2A restrains poised RNA polymerase II at bivalent genes in mouse ES cells. *Nat Cell Biol.* 9:1428-1435.
30. Ivey, K.N., Muth, A., Arnold, J., King, F.W., Yeh, R.F., Fish, J.E., Hsiao, E.C., Schwartz, R.J., Conklin, B.R., Bernstein, H.S., et al. 2008. MicroRNA regulation of cell lineages in mouse and human embryonic stem cells. *Cell Stem Cell.* 2:219-229.
31. Ventura, A., Young, A.G., Winslow, M.M., Lintault, L., Meissner, A., Erkeland, S.J., Newman, J., Bronson, R.T., Crowley, D., Stone, J.R., et al. 2008. Targeted deletion

reveals essential and overlapping functions of the miR-17 through 92 family of miRNA clusters. *Cell.* 132:875-886.
32. Rosa, A., Spagnoli, F.M., and Brivanlou, A.H. 2009. The miR-430/427/302 family controls mesendodermal fate specification via species-specific target selection. *Dev Cell.* 16:517-527.
33. Morin, R.D., O'Connor, M.D., Griffith, M., Kuchenbauer, F., Delaney, A., Prabhu, A.L., Zhao, Y., McDonald, H., Zeng, T., Hirst, M., et al. 2008. Application of massively parallel sequencing to microRNA profiling and discovery in human embryonic stem cells. *Genome Res.* 18:610-621.
34. Marson, A., Levine, S.S., Cole, M.F., Frampton, G.M., Brambrink, T., Johnstone, S., Guenther, M.G., Johnston, W.K., Wernig, M., Newman, J., et al. 2008. Connecting microRNA genes to the core transcriptional regulatory circuitry of embryonic stem cells. *Cell.* 134:521-533.
35. Boyer, L.A., Lee, T.I., Cole, M.F., Johnstone, S.E., Levine, S.S., Zucker, J.P., Guenther, M.G., Kumar, R.M., Murray, H.L., Jenner, R.G., et al. 2005. Core transcriptional regulatory circuitry in human embryonic stem cells. *Cell* 122:947-956.
36. Abu-Issa, R., Smyth, G., Smoak, I., Yamamura, K., and Meyers, E.N. 2002. Fgf8 is required for pharyngeal arch and cardiovascular development in the mouse. *Development* 129:4613-4625.
37. Liao, J., Aggarwal, V.S., Nowotschin, S., Bondarev, A., Lipner, S., and Morrow, B.E. 2008. Identification of downstream genetic pathways of Tbx1 in the second heart field. *Dev Biol.* 316:524-537.
38. Ryckebusch, L., Wang, Z., Bertrand, N., Lin, S.C., Chi, X., Schwartz, R., Zaffran, S., and Niederreither, K. 2008. Retinoic acid deficiency alters second heart field formation. *Proc Natl Acad Sci U S A.* 105:2913-2918. Epub 2008 Feb 2919.
39. Rochais, F., Dandonneau, M., Mesbah, K., Jarry, T., Mattei, M.G., and Kelly, R.G. 2009. Hes1 is expressed in the second heart field and is required for outflow tract development. *PLoS One.* 4:e6267.
40. von Both, I., Silvestri, C., Erdemir, T., Lickert, H., Walls, J.R., Henkelman, R.M., Rossant, J., Harvey, R.P., Attisano, L., and Wrana, J.L. 2004. Foxh1 is essential for development of the anterior heart field. *Dev Cell.* 7:331-345.
41. Chan, J.Y., Takeda, M., Briggs, L.E., Graham, M.L., Lu, J.T., Horikoshi, N., Weinberg, E.O., Aoki, H., Sato, N., Chien, K.R., et al. 2008. Identification of cardiac-specific myosin light chain kinase. *Circ Res.* 102:571-580.
42. Tomescot, A., Leschik, J., Bellamy, V., Dubois, G., Messas, E., Bruneval, P., Desnos, M., Hagege, A.A., Amit, M., Itskovitz, J., et al. 2007. Differentiation in vivo of cardiac committed human embryonic stem cells in postmyocardial infarcted rats. *Stem Cells* 25:2200-2205.
43. Colucci, F., Soudais, C., Rosmaraki, E., Vanes, L., Tybulewicz, V.L., and Di Santo, J.P. 1999. Dissecting NK cell development using a novel alymphoid mouse model: investigating the role of the c-abl proto-oncogene in murine NK cell differentiation. *J Immunol.* 162:2761-2765.
44. Sumi, T., Tsuneyoshi, N., Nakatsuji, N., and Suemori, H. 2008. Defining early lineage specification of human embryonic stem cells by the orchestrated balance of canonical Wnt/{beta}-catenin, Activin/Nodal and BMP signaling. *Development.* 135:2969-2979.
45. Naito, A.T., Shiojima, I., Akazawa, H., Hidaka, K., Morisaki, T., Kikuchi, A., and Komuro, I. 2006. Developmental stage-specific biphasic roles of Wnt/beta-catenin signaling in cardiomyogenesis and hematopoiesis. *Proc Natl Acad Sci U S A.* 103:19812-19817.

46. Zeineddine, D., Papadimou, E., Chebli, K., Gineste, M., Liu, J., Grey, C., Thurig, S., Behfar, A., Wallace, V.A., Skerjanc, I.S., et al. 2006. Oct-3/4 dose dependently regulates specification of embryonic stem cells toward a cardiac lineage and early heart development. *Dev Cell.* 11:535-546.
47. Boyer, L.A., Lee, T.I., Cole, M.F., Johnstone, S.E., Levine, S.S., Zucker, J.P., Guenther, M.G., Kumar, R.M., Murray, H.L., Jenner, R.G., et al. 2005. Core transcriptional regulatory circuitry in human embryonic stem cells. *Cell.* 122:947-956.
48. Greer Card, D.A., Hebbar, P.B., Li, L., Trotter, K.W., Komatsu, Y., Mishina, Y., and Archer, T.K. 2008. Oct4/Sox2-Regulated miR-302 Targets Cyclin D1 in Human ESC. *Mol Cell Biol* 18:18.
49. Kulisz, A., and Simon, H.G. 2008. An evolutionarily conserved nuclear export signal facilitates cytoplasmic localization of the Tbx5 transcription factor. *Mol Cell Biol.* 28:1553-1564. .
50. Bernex, F., De Sepulveda, P., Kress, C., Elbaz, C., Delouis, C., and Panthier, J.J. 1996. Spatial and temporal patterns of c-kit-expressing cells in WlacZ/+ and WlacZ/WlacZ mouse embryos. *Development.* 122:3023-3033.
51. Cai, C.L., Liang, X., Shi, Y., Chu, P.H., Pfaff, S.L., Chen, J., and Evans, S. 2003. Isl1 identifies a cardiac progenitor population that proliferates prior to differentiation and contributes a majority of cells to the heart. *Dev Cell.* 5:877-889.
52. Waldo, K.L., Kumiski, D.H., Wallis, K.T., Stadt, H.A., Hutson, M.R., Platt, D.H., and Kirby, M.L. 2001. Conotruncal myocardium arises from a secondary heart field. *Development* 128:3179-3188.
53. Morikawa, Y., and Cserjesi, P. 2008. Cardiac neural crest expression of Hand2 regulates outflow and second heart field development. *Circ Res* 103:1422-1429. Epub 2008 Nov 1413.
54. Stottmann, R.W., Choi, M., Mishina, Y., Meyers, E.N., and Klingensmith, J. 2004. BMP receptor IA is required in mammalian neural crest cells for development of the cardiac outflow tract and ventricular myocardium. *Development* 131:2205-2218. Epub 2004 Apr 2208.
55. Tomita, Y., Matsumura, K., Wakamatsu, Y., Matsuzaki, Y., Shibuya, I., Kawaguchi, H., Ieda, M., Kanakubo, S., Shimazaki, T., Ogawa, S., et al. 2005. Cardiac neural crest cells contribute to the dormant multipotent stem cell in the mammalian heart. *J Cell Biol* 170:1135-1146.
56. Seguchi, O., Takashima, S., Yamazaki, S., Asakura, M., Asano, Y., Shintani, Y., Wakeno, M., Minamino, T., Kondo, H., Furukawa, H., et al. 2007. A cardiac myosin light chain kinase regulates sarcomere assembly in the vertebrate heart. *J Clin Invest.* 117:2812-2824.
57. Meilhac, S.M., Esner, M., Kelly, R.G., Nicolas, J.F., and Buckingham, M.E. 2004. The clonal origin of myocardial cells in different regions of the embryonic mouse heart. *Dev Cell.* 6:685-698.
58. Maherali, N., Ahfeldt, T., Rigamonti, A., Utikal, J., Cowan, C., and Hochedlinger, K. 2008. A high-efficiency system for the generation and study of human induced pluripotent stem cells. *Cell Stem Cell.* 3:340-345.
59. Pfaffl, M.W. 2001. A new mathematical model for relative quantification in real-time RT-PCR. *Nucleic Acids Res* 29:e45.
60. Rucker-Martin, C., Pecker, F., Godreau, D., and Hatem, S.N. 2002. Dedifferentiation of atrial myocytes during atrial fibrillation: role of fibroblast proliferation in vitro. *Cardiovasc Res.* 55:38-52.
61. Nelson, J.D., Denisenko, O., and Bomsztyk, K. 2006. Protocol for the fast chromatin immunoprecipitation (ChIP) method. *Nat Protoc.* 1:179-185.

62. Dahl, J.A., and Collas, P. 2007. Q2ChIP, a quick and quantitative chromatin immunoprecipitation assay, unravels epigenetic dynamics of developmentally regulated genes in human carcinoma cells. *Stem Cells.* 25:1037-1046.
63. Li, Z., Lu, J., Sun, M., Mi, S., Zhang, H., Luo, R.T., Chen, P., Wang, Y., Yan, M., Qian, Z., et al. 2008. Distinct microRNA expression profiles in acute myeloid leukemia with common translocations. *Proc Natl Acad Sci U S A.* 105:15535-15540.

Figure legends

Figure 1: SSEA-1$^+$ cardiac progenitors: gene and protein profiles. ESCs were treated or not (CTRL) for 4 days with BMP2 (10ng/ml) and (**A**) monitored by flow cytometry using an anti-SSEA-1-FITC antibody, or (**B,C)** separated using the anti-SSEA-1 Miltenyi kit and the MACS columns. SSEA-1$^-$ and SSEA-1$^+$ cDNAs were run in real time PCR. Data are from 8 experiments performed on HUES-24 cell line and reproduced in different HESC lines (H9, HUES-9, HUES-24, HUES-26, I3 and I6). The inset in C illustrates SSEA-1$^+$ cells immunostained with anti-Tbx6 and -Mesp1/2 antibody 12-24 hours after sorting (**D,E**) Chromatin Immunoprecipitation assay using (**D**) anti-H3triMeK4, or -triMeK27 antibodies or (**E**) the anti-PolII or (inset) serine-phosphorylated PolII (Ser5-PPolII). Q-PCR was used to amplify the chromatin-bound DNA using primers specific for *Oct-4, Tbx6, Isl1, Mef2c , Nkx2.5, α-Actin* and *Pax4* promoters (sequence within the 700 bp in 3' of ATG, table2). Data (n=5) show fold enrichment of methylated histones on promoters in the SSEA-1$^+$ *vs* SSEA-1$^-$ population. The gels illustrate the specificity of PCR products (input, SSEA1$^+$ DNA samples from anti-triMeH3K4 IP, anti-rabbit IgG or no antibody). In E, the upper part of inset: PCR gel of DNA products following real time PCR indicates a complete loss of serine-phosphorylated PolII on both the *Nanog* and *sox2* promoters. ChiP experiments have been mostly performed using HUES-24 cell line and were validated in two other experiments using I6 cell line.

Figure 2: Heatmap representative of microRNA profile between SSEA-1$^+$ and SSEA-1$^-$ cells or HUES cells. Total RNA was extracted from HUES, SSEA-1$^+$ and SSEA-1$^-$ cells and hybridised to a miRNA microarray. Experiments were performed 6 times and log2 ratio values are shown in the heat map.

Figure 3: BMP2-induced SSEA-1$^+$ cardiac progenitors give rise to cardiac, endothelial and smooth muscle cells. (**A**) Cell clonogenicity: BMP2-induced SSEA-1$^+$ sorted cells were plated at different densities, 5000, 500, 50, 5 and 1 cell/well in 96 well-plates containing MEFs. Five days later, cells were stained with DAPI to be scanned using an arrayscan. Cell colonies were numbered using the Cellomics viewer software. Insets: colony generated from one single SSEA-1$^+$ cell and visualized 2 (right inset) or 5 (up-left inset) days later. Inset on the right: a single SSEA-1$^+$ cell derived from the HUES-9 pOct-4-GFP cell line was plated in a microwell of 96 well-plates and visualised by fluorescence right after plating (top image) or 5 days later (bottom GFP and transmitted light images). (**B**) Immunofluorescence of BMP2-induced SSEA-1$^+$ cells cultured for 5 days on MEF in the absence of growth factors or challenged by PDGF or VEGF, or co-cultured with human cardiac fibroblasts; up-left insets show magnification of localisation of markers. The inset in the actinin panel shows a magnification of sarcomeres. Experiments were done in triplicate with similar results. (**C**) BMP2-induced SSEA-1$^+$ cells cultured for 5 days on MEF immunostained with anti-Isl1, -Mef2c or -Nkx2.5 antibodies were quantified by High content cell imaging using an arrayscan. Numbers in the bars of the graph indicate the number of scored and validated cells. Images were acquired using a 20x magnification but panel SM myosin acquired at 40X magnification.

Figure 4: BMP2-induced SSEA-1$^+$ primate cardiac progenitors differentiate in mature cardiomyocytes. Immunostaining of actin-P EGFP SSEA-1$^+$ ORMES cultured on (**A,B,E**) both cardiac fibroblasts and myocytes (**A**) anti-GFP, anti-actinin on left images and merged image on the right); **(B)** anti-GFP immunostaining and dapi staining of nuclei of SSEA-1$^+$ cells; z-stacked of images was acquired in laser-scanning confocal microscope with the green

and blue channels together with differential interference contrast images. The merged image of a 200 nm focal plane is shown. (**C**) merged image anti-actinin (red) , -GFP (green) and Cx43 (white) immunostaining (**D**) actin-P EGFP SSEA-1^+ ORMES cultured on only cardiomyocytes (**E**) only fibroblasts. GFP in green, actinin in red, and Cx43 or phosphorylated P-Cx43 in white. (**F**) actin-P EGFP SSEA-1^+ ORMES cultured on both cardiac fibroblasts and myocytes immunostained with the anti-GFP (green in the left image), -actinin (red) and –MLC2v (blue) antibodies in the right image. These images are representative of 3 co-culture experiments. (G) actin-P EGFP SSEA-1^+ ORMES were cultured for 2 weeks on matrigel in the presence of filtered conditioned medium of a mix of fibroblasts and cardiomyocytes and actin stained with phalloïdin. (H) actin-P EGFP SSEA-1^+ ORMES cultured on both cardiac fibroblasts and myocytes immunostained with the anti--β-MHC (red in the left image), -GFP (green in the middle image). Merged image is shown on the right. The sarcomeric staining of GFP is due to its binding to myosin (60).

Figure 5: SSEA-1^+ cells safely engraft in infarcted primate myocardium (**A**) BMP2-induced gene expression in ORMES. (**B**) GFP expressing cells following engraftment of actin-P EGFP ORMES in the scar area of the myocardium. (**C**) teratoma formed following cell engraftment (the left and right images show low and high magnification, respectively).

(**D**) Flow cytometry analysis of SSEA-1-FITC positive ORMES (**E**) Q-PCR of mesodermal, cardiac genes (or pluripotency genes, inset) expressed in SSEA-1^+ cells sorted after 4 days BMP2 treatment. Data were normalised to GAPDH and to the SSEA-1^- population right after sorting. (**F**) Kinetic of gene expression in SSEA-1^+ cells expressed as fold changes *vs* SSEA-1^- cells normalised to undifferentiated ORMES-2 following 4 days BMP2 after sorting and following 7 days culture on MEF. (**G**) Eosin hematoxylin staining of myocardial section from a postinfarction primate having received the medium (left image, sham) or the cells together

(right image) with an image illustrating the low background of the green GFP fluorescence channel in the non cell-grafted myocardium (middle panel).

(**H**) Upper panels: from left to right, GFP-expressing cells 2 months following engraftment of actin-P EGFP and SSEA-1^+ ORMES. 40x magnification of a myocardial section; co-staining of actin-P EGFP and SSEA-1^+ ORMES with anti-CD31 and anti-SMA antibodies ; co-staining of actin-P EGFP and SSEA-1^+ ORMES with an anti-GFP, anti-actinin and anti-MLC2v antibodies (the inset shows co staining of GFP and MLCK in a myocardial section grafted with SSEA-1^+ ORMES).

Figure 6 Directed specification of pluripotent stem cells towards a cardiac fate. BMP2-induced Oct-4^+, SSEA1^+ cells give rise to endo/mesendodermal cells secreting cardiogenic factors further directing the cell fate toward a cardiac phenotype when plated on MEF releasing FGF2. Addition of PDGF or VEGF directs the fate of cells toward a smooth muscle and endothelial phenotype, respectively.

Cell Line	% BMP-2-induced SSEA-1cells
HUES-24	49±9 (n=20)
HUES-26	20±5 (n=3)
HUES-9	53±5 (n=5)
I6	49±6 (n=7)
H9	60±8 (n=5)
iPS	30±5 (n=4)

Table 1 : Yield of SSEA-1^{+} cell sorting using anti-SSEA-1 conjugated magnetic beads

GENES	**Real time PCR**	
	Forward 5'-3'	**Reverse 5'-3'**
GAPDH	ATGGGCAAGGTGAAGGTCGGAG	TCGCCCGACTTGATTTTGCAGG
PLURIPOTENCY		
Oct-4iA	CTCCTGGAGGGCCAGGAATC	CCACATCGGCCTGTGTATAT
Nanog	CAAAGGCAAACAACCCACTT	TCTGCTGGAGGCTGAGGTAT
LeftyA	GGGAATTGGGATACCTGGATTC	TAAATATGCACGGGCAAGGCTC
TDGF1	ACAGAACCTGCTGCCTGAAT	ATCACAGCCGGGTAGAAATG
ECTODERM NEURAL CREST		
Nestin	GGCAGCGTTGGAACAGAGGT	TGGATGCAGGGATGATGTTC
Sox1	CCTCGGATGTCTGGTCAAGT	TAGACAGCCGGCAGTCATAC
Pax3	GCCAATCAACTGATGGCTTT	GAAGGAATCGTGCTTTGGTG
ENDODERM		
Sox17	GGCGCAGCAGAATCCAGA	CCACGACTTGCCCAGCAT
Hex	CTCCAACGACCAGACCATCG	CCTGTCTCTCGCTGAGCTGC
Foxa	AGCAGGCGCCCAGCAAGATG	TGGCGGCGCAAGTAGCAG-
MESODERM		
Brachyury	CGGAACAATTCTCCAACCTATT	GTACTGGCTGTCCACGATGTCT-
Flk1	GCATCTCATCTGTTACAGC	CTTCATCAATCTTTACCCC
Tbx6	AGGCCCGCTACTTGTTTCTTCTGG	TGGCTGCATAGTTGGGTGGCTCTC
CARDIAC		
Mesp1	CTCTGTTGGAGACCTGGATG	CCTGCTTGCCTCAAAGTG
Tbx5	TACCACCACACCCATCAAC	ACACCAAGACAGGGACAGAC
Tbx18	GGGTTTGGAAGCCTTGGTGG	GGCAGAATAGTCAGCAGGGG
GATA4	GCATCAACCGGCCGCTCATCA	GGTTCTTGGGCTTCCGTTTTCT
Nkx2.5	CATTTACCCGGGAGCCTACG	GCTTTCCGTCGCCGCCGTGCGCGTG
Mef2c	AGATACCCACAACACACCACGCGCC	ATCCTTCAGAGAGTCGCATGC
c-Actin	CTATGTCGCCCTGGATTTTGAGAA	TGAGGGAAGGTGGTTTGGAAGAC
SMOOTH MUSCLE		
Myocardin	TTTCAGAGGTAACACAGCCTCCATCC	ACTGTCGGTGGCATAGGGATCAAA
CARDIAC 2ndary Heart lineage		
Isl1	CGCGTGCGGACTGTGCTGAAC	TTGGGCTGCTGCTGCTGGAGT
Tbx20	CTGAGCCACTGATCCCCACCAC	CTCAGGATCCACCCCCGAAAAG
RALDH2	CATGAACCCATCGGAGTGTGT	CTGGAGCAATCTTCCATGCAA
Tbx1	CGCAGTGGATGAAGCAAATCGTG	TTTGCGTGGGTCCACATAGACC
Hes1	GGAAATGACAGTGAAGCACCTCC	GAAGCGGGTCACCTCGTTCATG
PROMOTERS ChIP		
Oct4	GGCGAGTGGGGGGAGAAACTGA	GGCCTGGTGGGAGGAA
Sox2	ATTAGTCTGCTCTTCCTCGGAATGGTTGG	TGATGCTTGTTAAAAACGCTTCGCTCC
Nanog	GTTCTGTTGCTCGGTTTTCT	TCCCGTCTACCAGTCTCACC
Tbx6	TAACCCGTTCCTGCCCCACCTG	TCCGCTTGAGCTCCCCCTTCC
Isl1	CGGAGGAGCAGCGCCACAGGAG	GGCGAGCCAGCGGGAGAGGATT
Mef2c	GGGGCAAAGCTTCGGTGTTC	AGTGCCTTTCTGCTTCTCCA
Nkx2.5	CAGTCTTGGGAGCTCAAGACT	CAGATCCCCAAGCTTACTAGC
c-Actin	CTATTTGGCCATCCCCCTGACTGC	GGGCCGCTTTATAGAACGCTGATG
Pax4	CACACTGTGGCTCCTTCCTC	GGGTGCTCATAGGGAAAACA

Table 2: PCR primer sequences

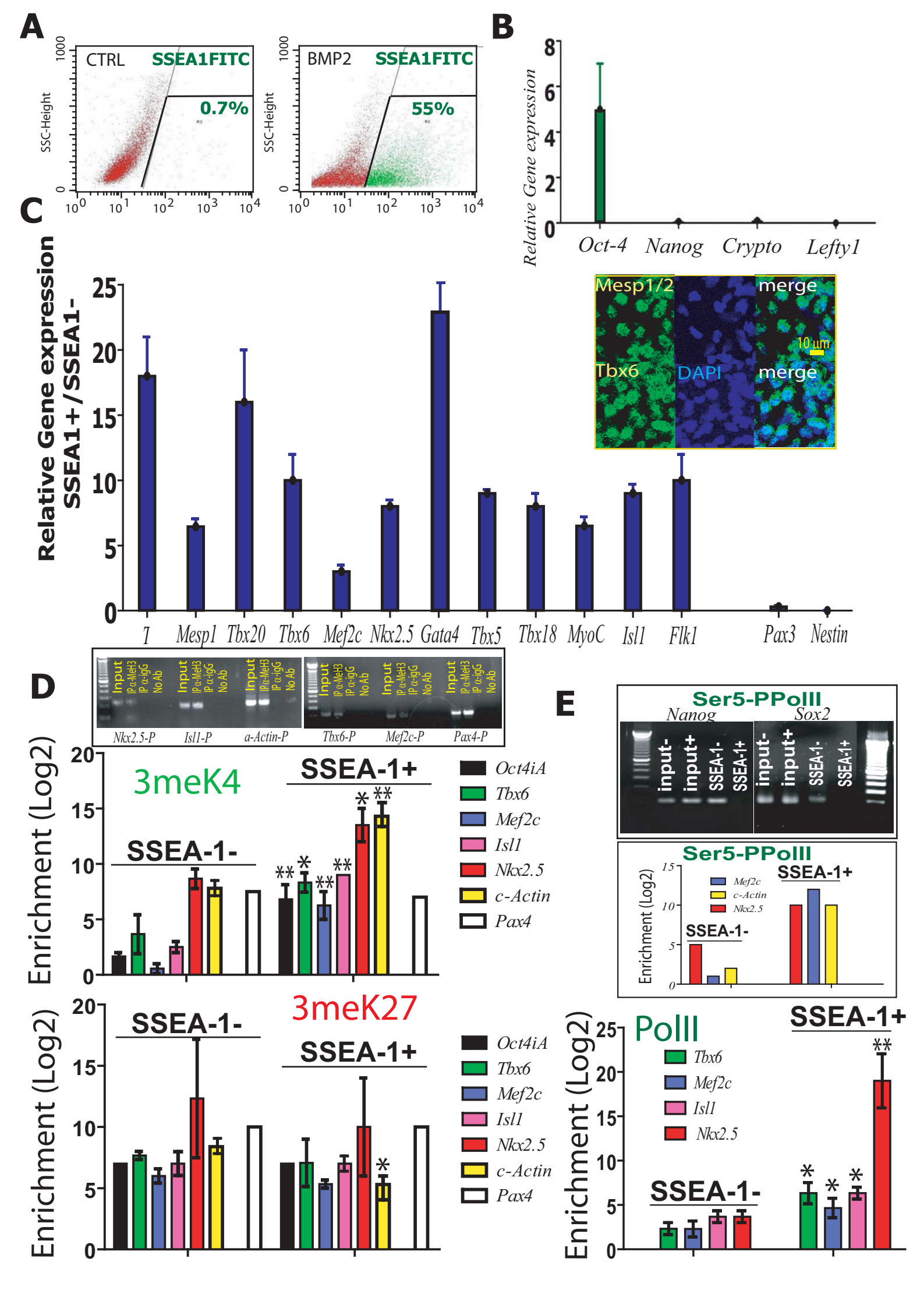
A
CTRL
SSEA1FITC
0.7%
BMP2
SSEA1FITC
55%
SSC-Height
B
Relative Gene expression
Oct-4
Nanog
Crypto
Lefty1
C
Relative Gene expression
SSEA1+/SSEA1-
1
Mesp1
Tbx20
Tbx6
Mef2c
Nkx2.5
Gata4
Tbx5
Tbx18
MyoC
Isl1
Flk1
Pax3
Nestin
Mesp1/2
Tbx6
DAPI
merge
10 µm
D
Nkx2.5-P
Isl1-P
a-Actin-P
Tbx6-P
Mef2c-P
Pax4-P
3meK4
SSEA-1-
SSEA-1+
Enrichment (Log2)
Oct4iA
Tbx6
Mef2c
Isl1
Nkx2.5
c-Actin
Pax4
3meK27
E
Ser5-PPolII
Nanog
Sox2
input-
input+
SSEA-1-
SSEA-1+
PolII

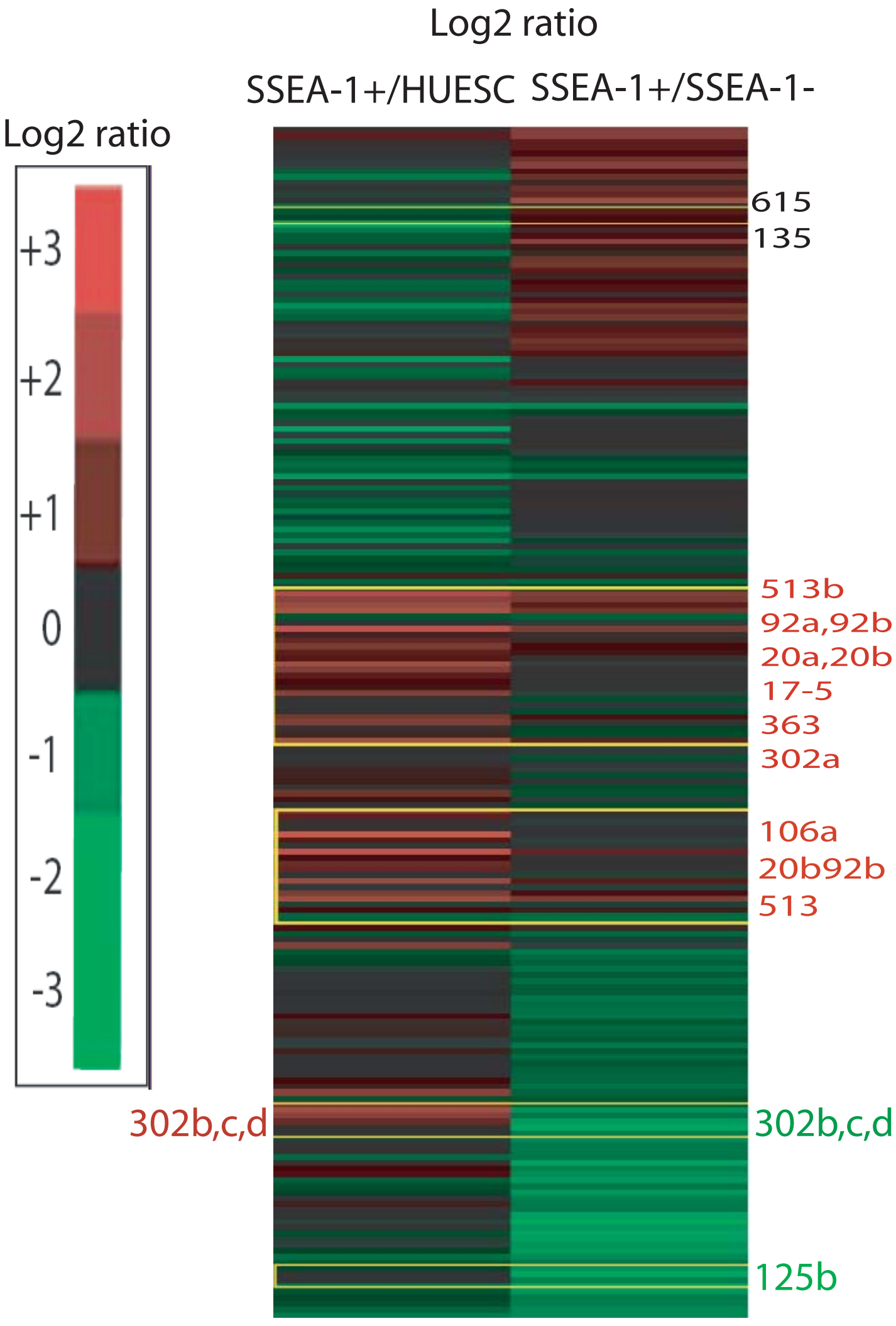
Log2 ratio
SSEA-1+/HUESC
SSEA-1+/SSEA-1-
Log2 ratio
+3
+2
+1
0
-1
-2
-3
615
135
513b
92a,92b
20a,20b
17-5
363
302a
106a
20b92b
513
302b,c,d
302b,c,d
125b

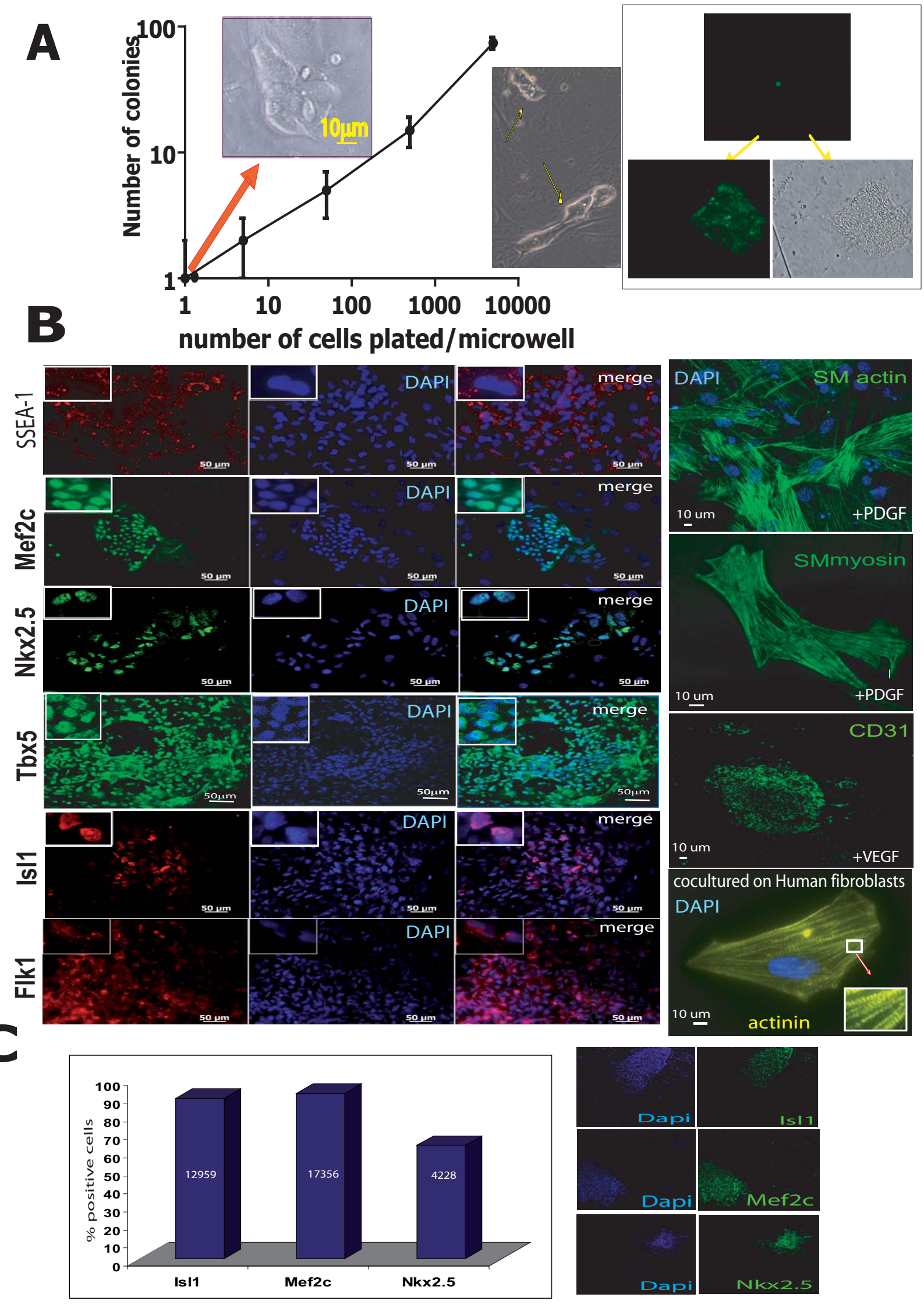
A
Number of colonies
100
10
1
1
10
100
1000
10000
number of cells plated/microwell
10µm
B
SSEA-1
Mef2c
Nkx2.5
Tbx5
Isl1
Flk1
DAPI
merge
50 µm
50µm
DAPI
SM actin
10 um
+PDGF
SMmyosin
10 um
+PDGF
CD31
10 um
+VEGF
cocultured on Human fibroblasts
DAPI
10 um
actinin
% positive cells
100
90
80
70
60
50
40
30
20
10
0
12959
17356
4228
Isl1
Mef2c
Nkx2.5
Dapi
Isl1
Dapi
Mef2c
Dapi
Nkx2.5

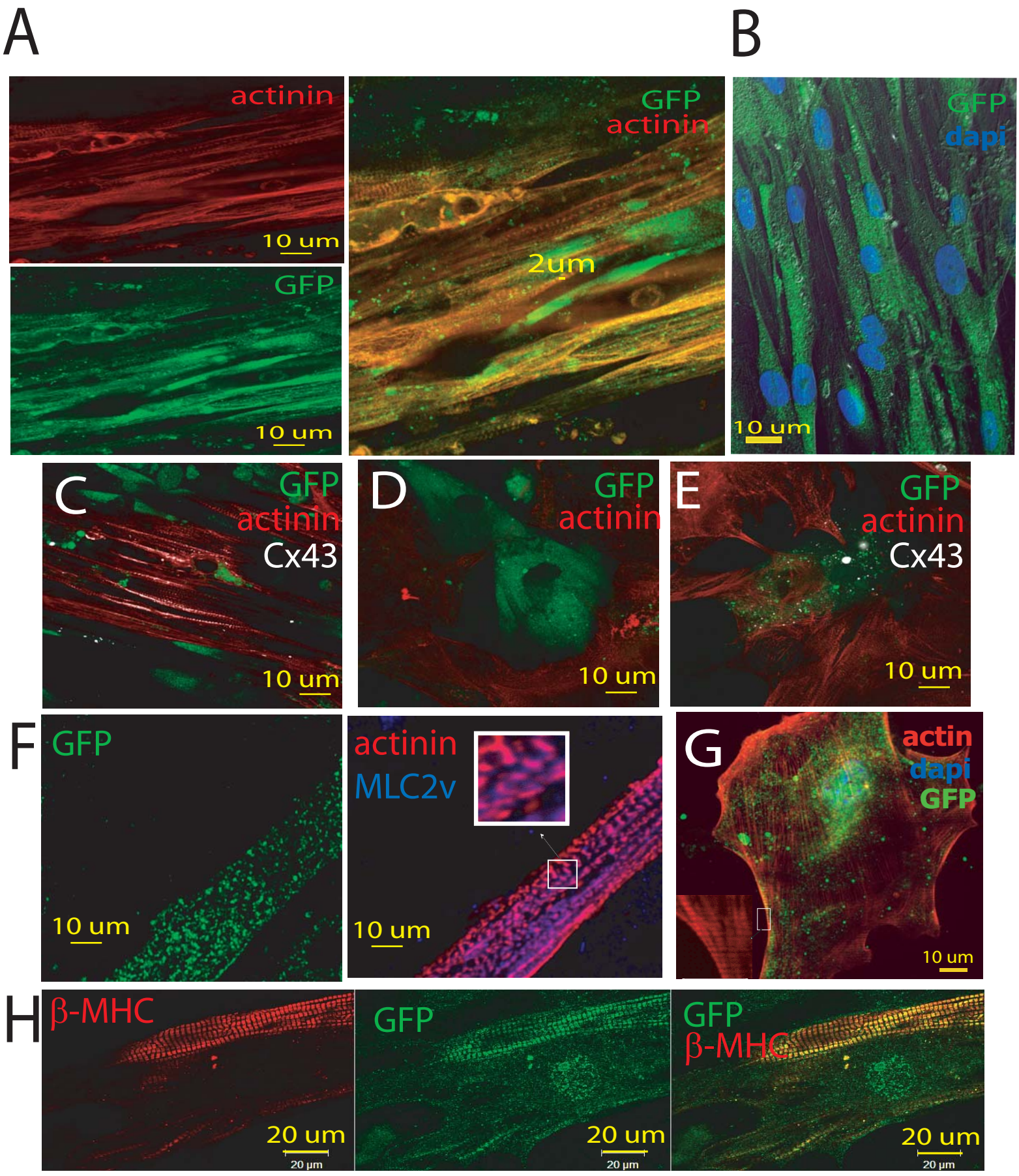
A
actinin
10 um
GFP
10 um
GFP
actinin
2um
B
GFP
dapi
10 um
C
GFP
actinin
Cx43
10 um
D
GFP
actinin
10 um
E
GFP
actinin
Cx43
10 um
F
GFP
10 um
actinin
MLC2v
10 um
G
actin
dapi
GFP
10 um
H
β-MHC
20 um
20 µm
GFP
20 um
20 µm
GFP
β-MHC
20 um
20 µm

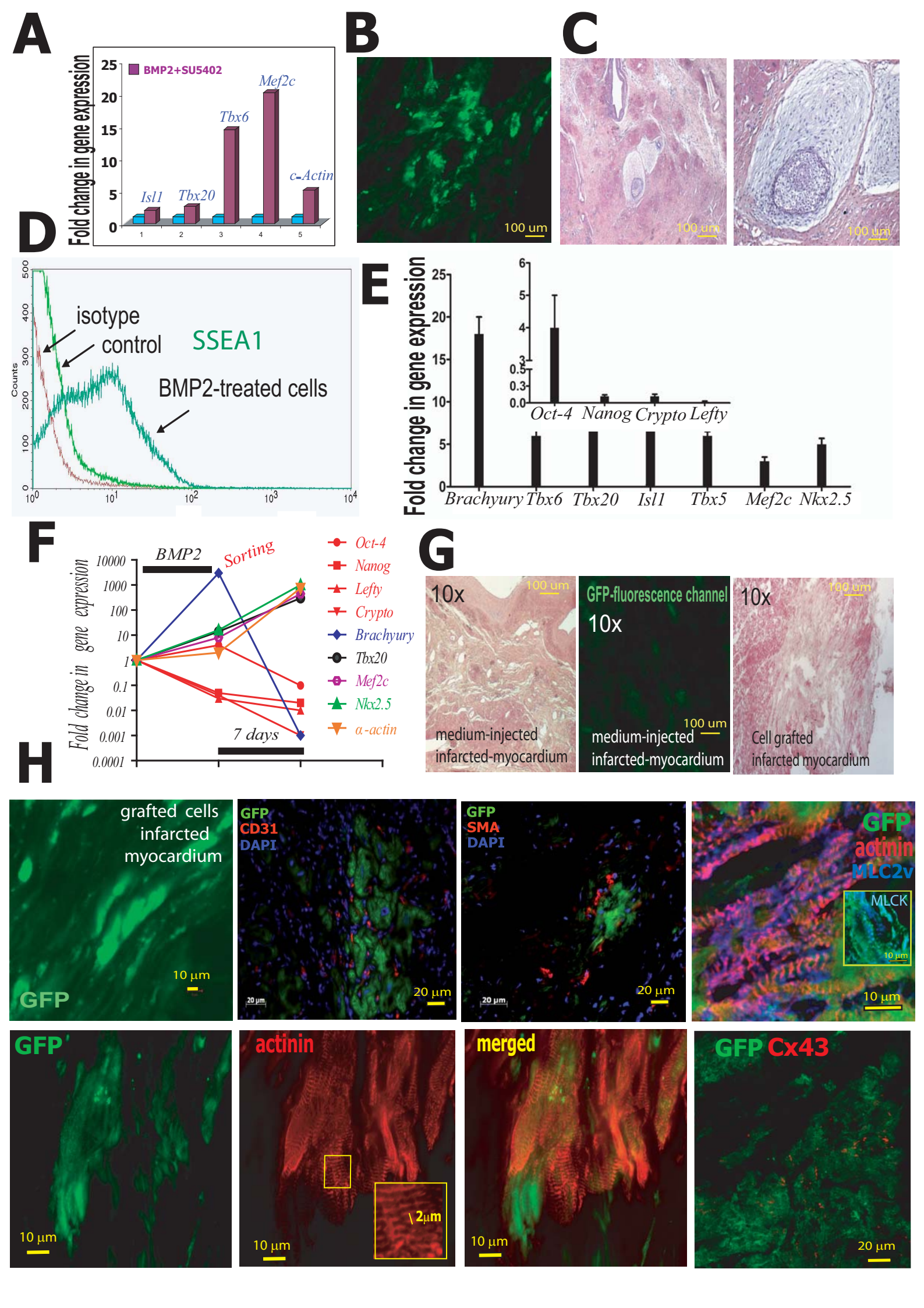
A
Fold change in gene expression
BMP2+SU5402
Isl1
Tbx20
Tbx6
Mef2c
c-Actin
B
100 um
C
100 um
100 um
D
isotype control
SSEA1
BMP2-treated cells
Counts
E
Fold change in gene expression
Oct-4
Nanog
Crypto
Lefty
Brachyury
Tbx6
Tbx20
Isl1
Tbx5
Mef2c
Nkx2.5
F
BMP2
Sorting
7 days
Fold change in gene expression
Oct-4
Nanog
Lefty
Crypto
Brachyury
Tbx20
Mef2c
Nkx2.5
α-actin
G
10x
100 um
medium-injected infarcted-myocardium
GFP-fluorescence channel
10x
100 um
medium-injected infarcted-myocardium
10x
100 um
Cell grafted infarcted myocardium
H
grafted cells infarcted myocardium
GFP
10 μm
GFP
CD31
DAPI
20 μm
GFP
SMA
DAPI
20 μm
GFP
actinin
MLC2v
MLCK
10 μm
10 μm
GFP
10 μm
actinin
2μm
10 μm
merged
10 μm
GFP Cx43
20 μm

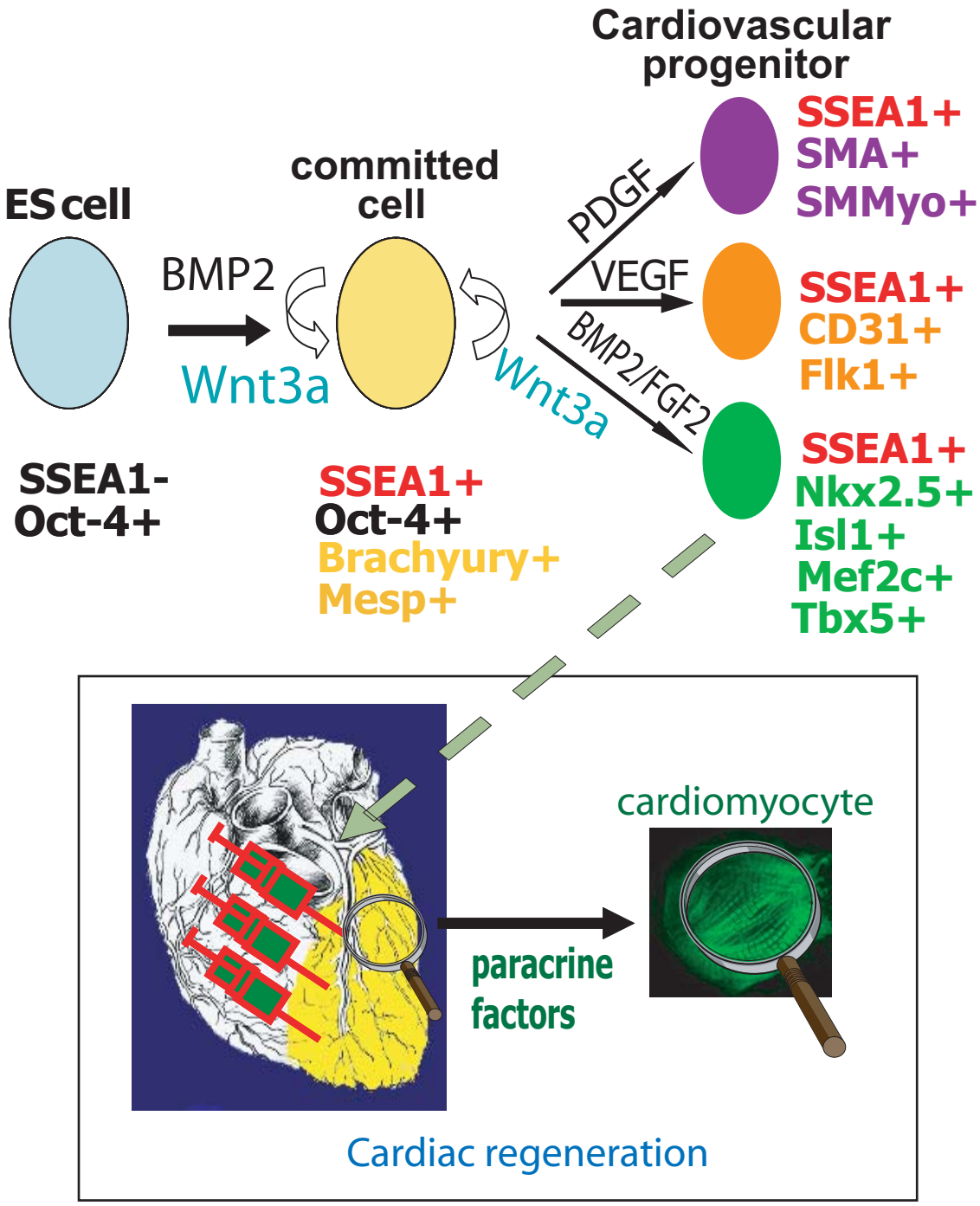
Cardiovascular progenitor
SSEA1+
SMA+
SMMyo+
committed cell
ES cell
PDGF
BMP2
VEGF
SSEA1+
CD31+
Flk1+
Wnt3a
Wnt3a
BMP2/FGF2
SSEA1+
Nkx2.5+
Isl1+
Mef2c+
Tbx5+
SSEA1-
Oct-4+
SSEA1+
Oct-4+
Brachyury+
Mesp+
cardiomyocyte
paracrine factors
Cardiac regeneration

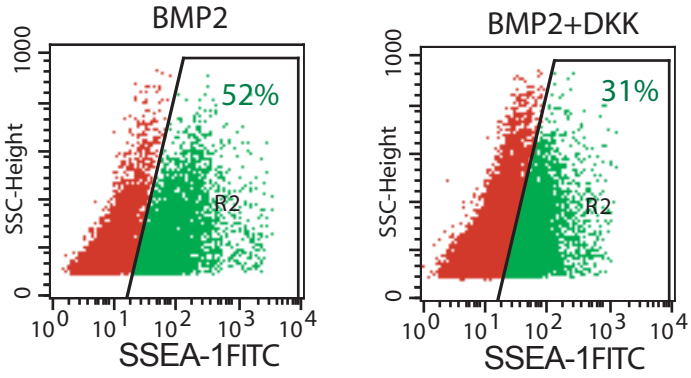
BMP2
SSC-Height
1000
0
52%
R2
10^0 10^1 10^2 10^3 10^4
SSEA-1FITC
BMP2+DKK
SSC-Height
1000
0
31%
R2
10^0 10^1 10^2 10^3 10^4
SSEA-1FITC

supl Fig1

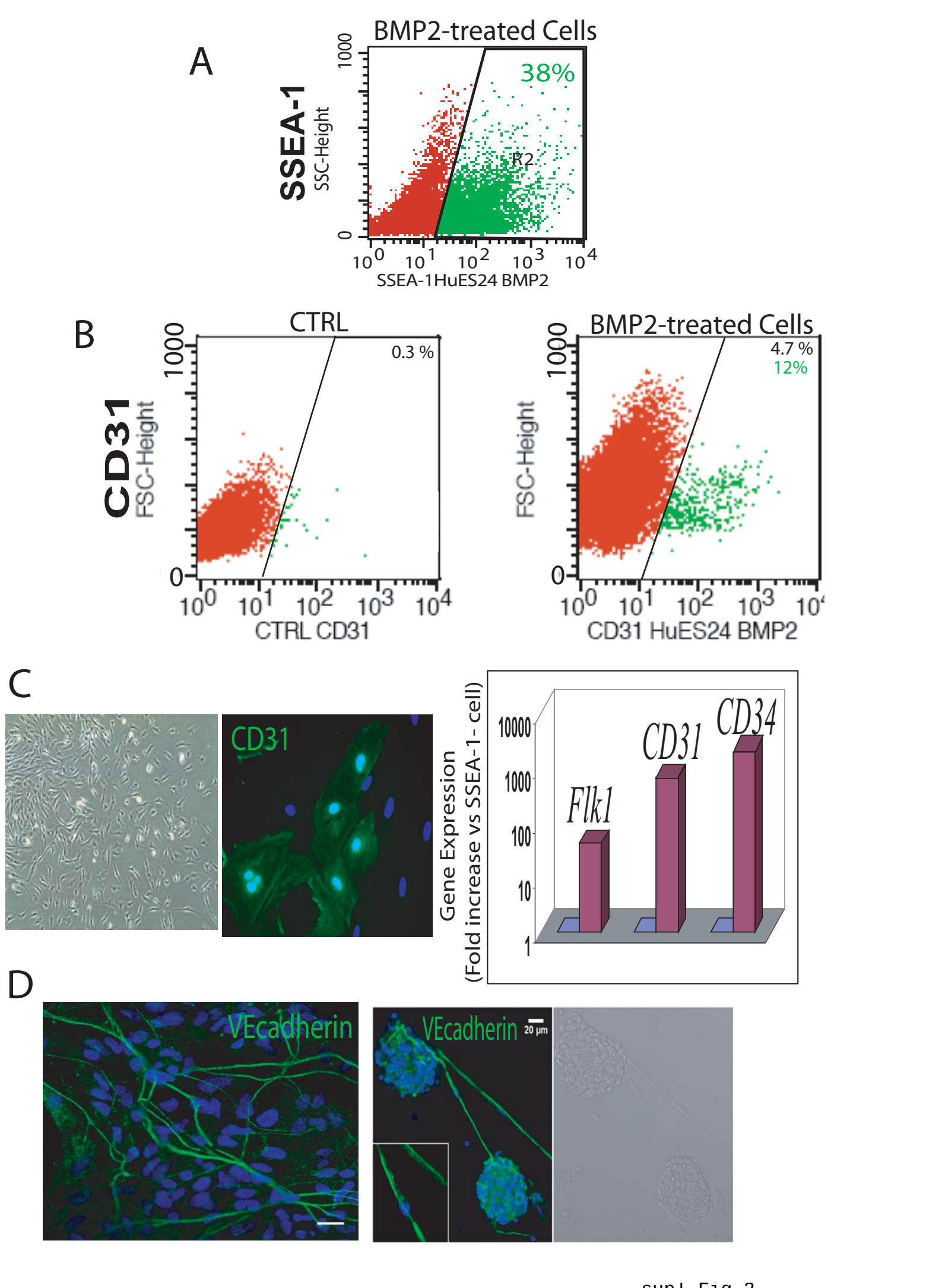
A
BMP2-treated Cells
SSEA-1
SSC-Height
1000
0
38%
R2
10^0 10^1 10^2 10^3 10^4
SSEA-1HuES24 BMP2
B
CTRL
CD31
FSC-Height
1000
0
0.3 %
10^0 10^1 10^2 10^3 10^4
CTRL CD31
BMP2-treated Cells
FSC-Height
1000
0
4.7 %
12%
10^0 10^1 10^2 10^3
CD31 HuES24 BMP2
C
CD31
Gene Expression
(Fold increase vs SSEA-1- cell)
10000
1000
100
10
1
Flk1
CD31
CD34
D
VEcadherin
VEcadherin
20 µm

supl Fig 2

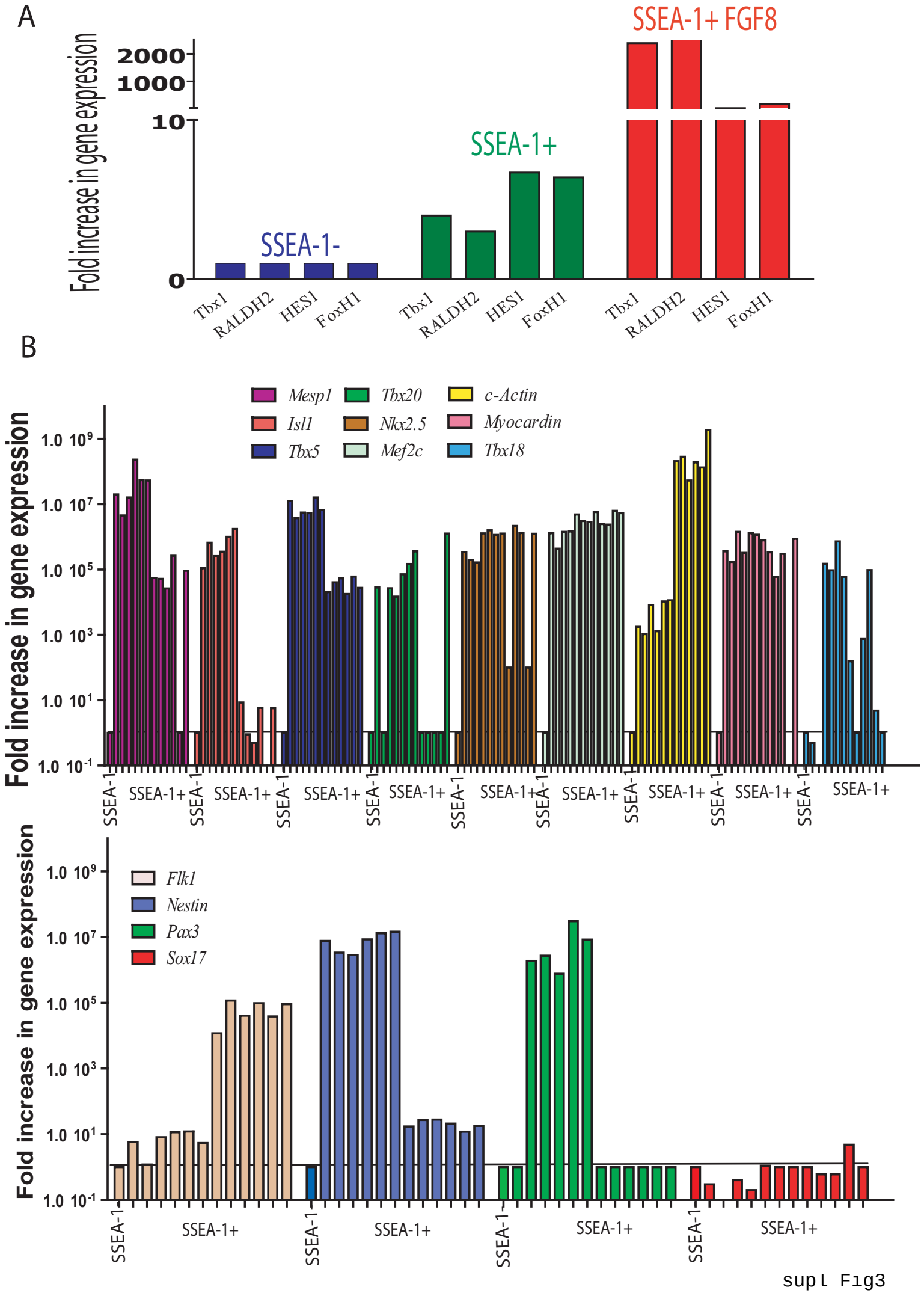
A
Fold increase in gene expression
2000
1000
10
0
SSEA-1-
SSEA-1+
SSEA-1+ FGF8
Tbx1
RALDH2
HES1
FoxH1
B
Fold increase in gene expression
Mesp1
Isl1
Tbx5
Tbx20
Nkx2.5
Mef2c
c-Actin
Myocardin
Tbx18
1.0 10^9
1.0 10^7
1.0 10^5
1.0 10^3
1.0 10^1
1.0 10^-1
SSEA-1-
SSEA-1+
Flk1
Nestin
Pax3
Sox17

supl Fig3

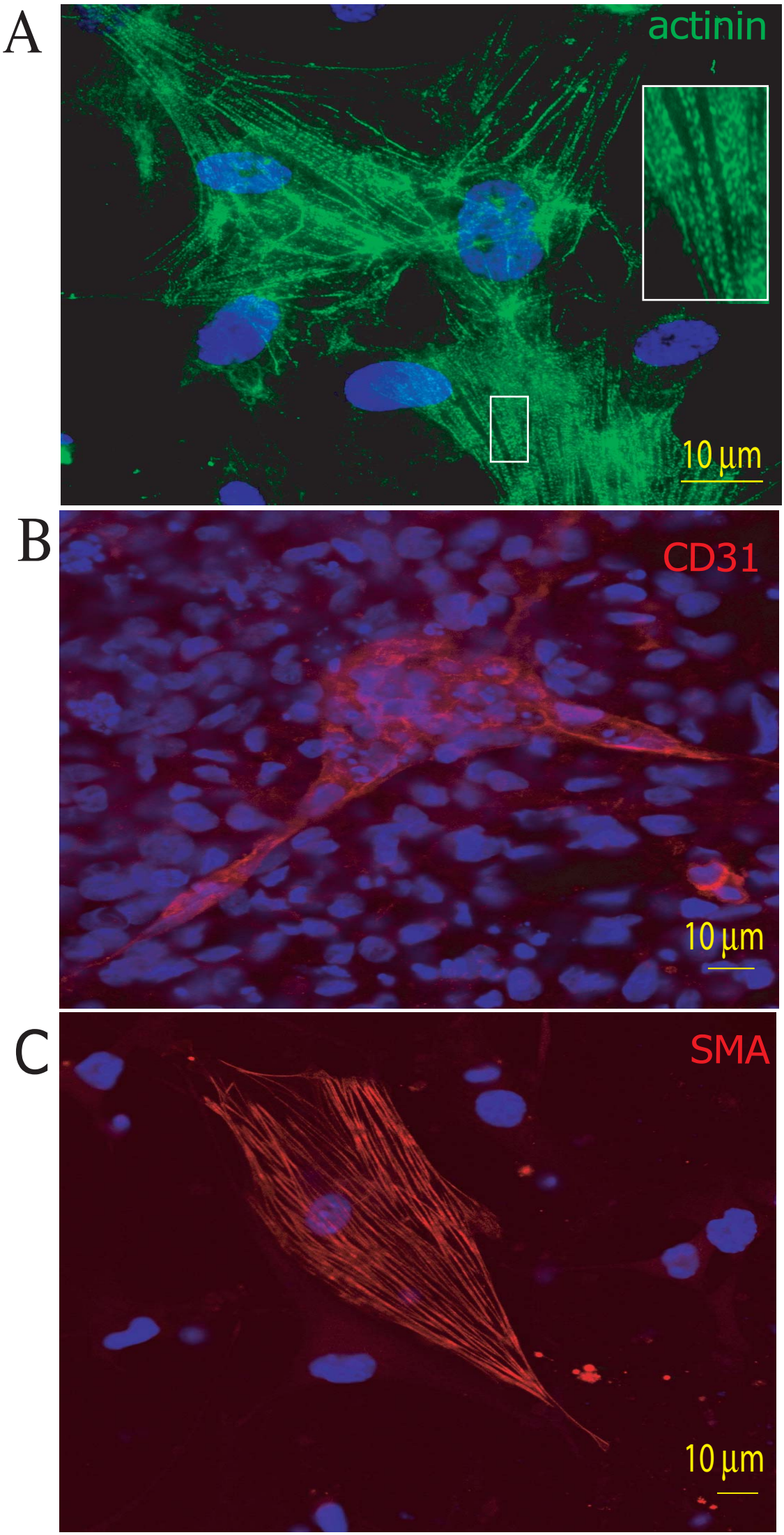

supl Fig 4

A

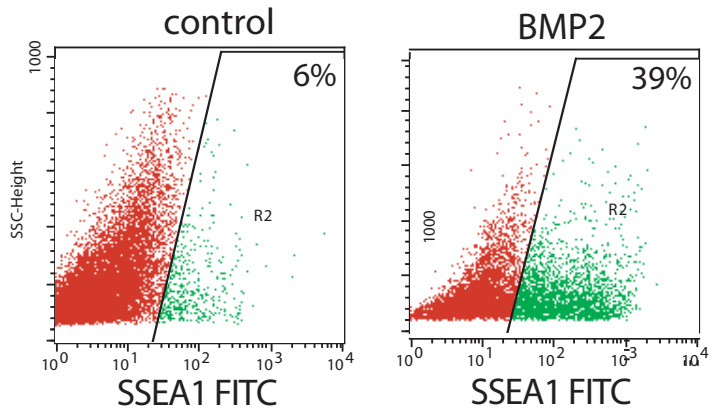
control
6%
R2
SSC-Height
SSEA1 FITC
BMP2
39%
R2
SSEA1 FITC

B

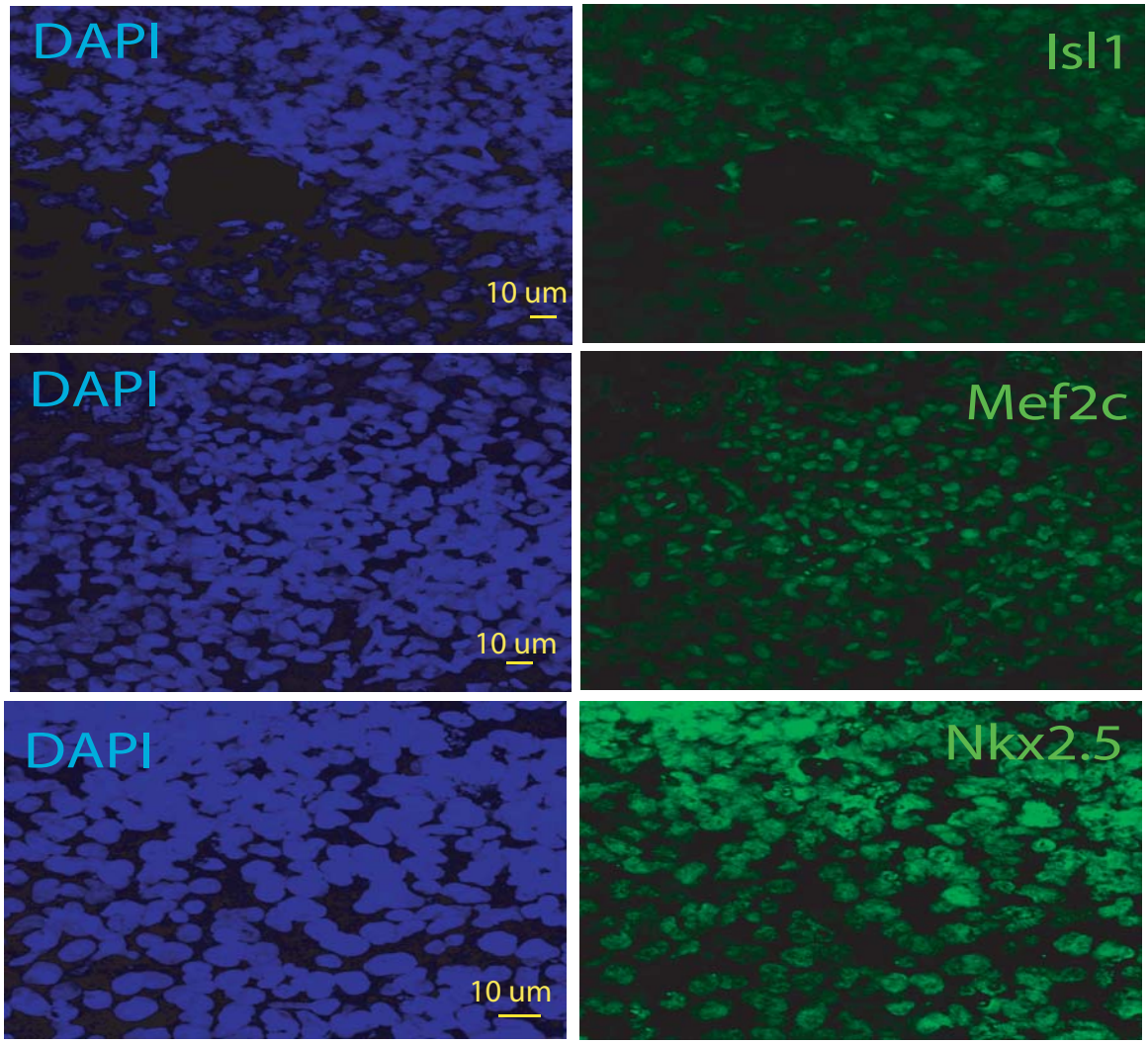
DAPI
10 um
Isl1
DAPI
10 um
Mef2c
DAPI
10 um
Nkx2.5

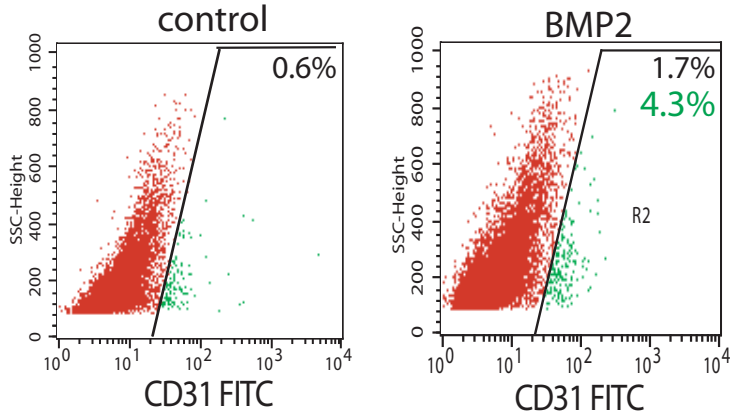
control
0.6%
SSC-Height
CD31 FITC
BMP2
1.7%
4.3%
R2
SSC-Height
CD31 FITC

Supl Fig 5

Supplementary Figure 1: DKK1 prevents BMP2-induced generation of SSEA-1$^+$ cardiac progenitors. Human ESCs were treated for 4 days with BMP2 alone or together with DKK and monitored by flow cytometry using the anti-FITC/SSEA-1 antibody. The experiment was performed in duplicate.

Supplementary Figure 2: Flow cytometry analysis of SSEA-1$^+$ cells (**A**) using an anti-CD31 antibody (**B**); gates were set as a function of control undifferentiated (SSEA-1 negative) cells. The percentage in green indicates the percentage of positive cells normalised to the percentage of SSEA-1+ cells. (**C**) SSEA-1$^+$ sorted cells were cultured for one week on MEF and then plated for 10 days on collagen-I-coated dishes and treated with VEGF (50ng/ml). The images show the morphology of cells and an anti-CD31 immunostaining and the graph, the real time PCR quantitation of Flk1, CD31 and CD34 mRNAs levels normalised to HUES SSEA-1 negative cells. (**D**) SSEA-1$^+$ sorted cells were plated for 10 days on collagen IV and challenged by VEGF. Formation of capillaries (left image) is evidenced by anti-VE cadherin immunostaing and cell morphology (right images).

Supplementary Figure 3: (A) Real time PCR monitoring of gene expression in SSEA-1$^-$ and SSEA-1$^+$ sorted cells and in SSEA-1$^+$ cells stimulated for 4 days with FGF8 **(B)** Real time PCR monitoring of gene expression in single colonies. SSEA-1$^+$ single colonies cultured for one week on MEF were picked-up randomly and RNA extracted. Expression of genes was monitored by real-time PCR. Results are normalised to GAPDH expression and SSEA-1$^-$ cells. The first bar from each gene indicates gene expression in SSEA1$^-$ cells and the following are SSEA-1$^+$ colonies from 1 to 12 in the same order for all genes.

Supplementary Figure 4 : a single clone of SSEA-1$^+$ cardiovascular progenitors give rise to cardiomyocytes (upper panel) when cultured on human fibroblasts (inset: magnification of sarcomeres), endothelial CD31$^+$ cells (middle panel) when cultured on collagen 1 and treated for one week with VEGF and SMA$^+$ smooth muscle cell (bottom panel) when cultured on collagen 1 and treated with PDGF. This experiment was repeated with 5 separate clones.

Supplementary Figure 5: iPS cells give rise to SSEA-1$^+$ cardiovascular progenitors.

iPS cells challenged with BMP2 expressed SSEA-1 (**A**) and CD31 (**B**) monitored by flow cytometry as well as 3 cardiac-restricted markers (Isl1, Mef2c, Nkx2.5) following one week of culture on MEF. In the CD31 panel, the percentage in green indicates the percentage of positive cells normalised to the percentage of SSEA-1$^+$ cells. The scale bars indicate 10 µm.